Assessment of Ferrate for Pre-Oxidation Treatment of Harmful Algal Blooms in Drinking Water Treatment

by

Kyle T. Gerlach Jr.

A Thesis Submitted to the Faculty of the Worcester Polytechnic Institute in partial fulfillment of the requirements for the Degree of Master of Science in Environmental Engineering by

_____

Kyle T. Gerlach Jr.

December 2019

APPROVED:

_____

Dr. Jeanine D. Dudle, Advisor

Committee Members:
Professor Jeanine D. Dudle
Professor John A. Bergendahl

Abstract

Harmful algal blooms in surface water supply systems pose a threat to public health and are increasing in both frequency and geographical distribution. Cyanobacteria can contribute to taste and odor issues and potentially release harmful cyanotoxins into the water. Several treatment methods are currently employed to control these blooms, including physical separation and chemical pre-oxidation. However, existing oxidation options can be costly; increase the release of intracellular material causing the formation of disinfection byproducts; or disrupt coagulation and filtration processes. This study investigated ferrate (Fe(VI)) as an alternative to other oxidants by measuring its effect on algae cells. Fe(VI) has several advantages as an oxidant, including a high oxidation potential, a low potential for harmful disinfection byproduct production, and formation of Fe(III) - which can potentially be beneficial for downstream treatment processes. Bench scale studies were conducted with laboratory prepared waters containing the common cyanobacteria *Microcystis aeruginosa* to examine the interactions between Fe(VI) and algae. The effects of ferrate oxidation on algae were characterized by particle counts, UV_{254} absorbance, total organic carbon (TOC) and dissolved organic carbon (DOC), and total nitrogen. Ferrate decomposition was also monitored. Results showed that Fe(VI) lysed algal cells under some conditions, but further oxidation of released organic matter is possible at some doses. Additionally, some coagulation benefits were observed through an overall decrease in total particle counts and an increase in particle sizes. In general, the results indicate that Fe(VI) could be a possible alternative to other oxidants for water utilities during harmful algal blooms; however, the final fate of resulting organic matter and the potential for disinfection byproduct formation should be further studied.

Acknowledgements

Table of Contents

List of Figures

List of Tables

Chapter 1: Background

1.1 Introduction

Harmful algal blooms are growing in frequency and distribution across the country and pose a major threat to water quality, aquatic ecosystems, and public health (Anderson et al., 2002). Of particular concern are blooms of cyanobacteria (blue-green algae) in drinking water sources, which can impart toxins such as microcystin-LR into the water (He et al., 2016). In addition, bloom events are commonly followed by bottom water anoxia, benthic animal mortalities, and general fish kills. A clear link has been established between the occurrence of toxic cyanobacterial blooms in lakes and (1) low level freshwater flowrates and (2) nutrient loading (especially phosphorous and nitrogen) (Anderson et al., 2002).

For example, agricultural runoff containing high levels of nitrogen and phosphorus fertilizer has caused large scale toxic algal blooms to occur in Lake Erie since the 1990s. One of the largest blooms to occur was in 2011, when 1,920 square miles of the lake (nearly 20%) was covered with a thick algae mat (Dybas, 2019). The most dangerous bloom occurred in 2014, when high concentrations of the cyanotoxin microcystin were detected in the finished water of the City of Toledo, Ohio water treatment plant. As a result, a "Do Not Use" order was declared for the City's water supply system, which serves 500,000 people. Additional large scale blooms occurred in 2013, 2014, 2015, 2017, and 2019. These blooms received a rating of 8 or higher on the 10 point scale developed by the National Oceanic and Atmospheric Administration (NOAA) and were all in the upper regions of the 'significant' category (NOAA, 2019).

These recent bloom occurrences have crippled the multi-billion dollar tourism industry, specifically impacting sport fishing and lake recreation. The benthic dead-zone created by algal blooms has also caused a decline in deepwater fish populations, such as perch and walleye (*Nature*, 2014). Future increases in anthropogenic nutrient loading from development around drinking water sources could cause similar scale blooms to occur in more widespread locations and could increases bloom frequency and severity. This would represent a major public health issue for those communities.

1.2 Problems Caused by Algae

Apart from the impacts on aquatic life and the source water environment, cyanotoxins and other cellular material released by algae cells during bloom formation pose health risks to consumers of public drinking water. As discussed by He et al. (2016), there are four classes of cyanotoxins that impact drinking waters. These four classes include cylindrospermopsin, anatoxin, saxitoxin, and microcystins. This report focuses on the cyanobacteria species *Microcystis aeruginosa* (*M. aeruginosa*) and one of its associated cyanotoxins, microcystin-LR.

Microcystins are not believed to be a defensive mechanism of algae cells but rather are released under oxidative stresses and nutrient deficiencies witnessed by the cell (Pimentel, 2016). These toxins are stable, non-volatile, water soluble, cyclic polypeptides generally consisting of a seven amino acid ring (He et al., 2016). These properties make algal toxins persistent in the environment and difficult to treat with conventional treatment methods.

While acute toxicity is the most obvious problem in cyanotoxin poisoning, the World Health Organization (WHO) has determined that long-term exposure at low concentrations may also pose a risk to public health (WHO, 1999). A chronic low-level exposure may cause adverse health effects, mainly carcinogenesis and tumor growth promotion in the liver, as witnessed in animal experimentation (WHO, 1999). Microcystins are believed to accumulate in the liver, brain, testes, lungs, kidneys, placenta, and other tissues, where they bind to serine/threonine protein phosphatases (Campos, 2010). Once bound to these compounds, microcystin acts as an inhibitor for this group of enzymes within the cell. It also induces oxidative stress in animal cells, which coupled with the inhibition of protein phosphatases, is the main mechanism of their toxicity (Campos, 2010).

In addition to microcystins, algal cells contain algal organic matter (AOM) which is made up of intracellular organic matter (IOM) and extracellular organic matter (EOM). Algae IOM is often rich in nitrogen organic matter (org-N). Algal cells can also carry surface-absorbed organic matter, including EOM and natural organic matter (NOM). These varying forms of organic material, especially the org-N matter, greatly contribute to the formation of disinfection byproducts (DBPs) during disinfection treatment processes with chlorine. Chlorinated org-N material can form nitrogenous DBPs, whose genotoxicity and carcinogenicity are two to three orders of magnitude higher than those of halogenated DBPs like trihalomethanes (THMs) and haloacetic acids (HAAs) (Xie et al., 2013).

1.3 Regulation of Cyanotoxins

Currently, the United States Environmental Protection Agency (EPA) has not established federal standards for cyanotoxins in drinking water. However, the EPA has included either cyanobacteria or their toxins on the Contaminant Candidate List (CCL) since 1998. In 2016, the cyanotoxin microcystin was specifically listed for the first time on the CCL4. The EPA has also required the monitoring of cyanotoxins in drinking water between 2018 and 2020, as part of the fourth round of the Unregulated Contaminant Monitoring Rule (UCMR 4).

Health Advisory (HA) levels for the cyanotoxins cylindrospermospsin and microcystin were established by the EPA in 2015. Although these HA levels are not regulations or legally enforceable, they provide guidance for levels below which adverse health effects are not anticipated to occur over specific exposure durations. The ten day Drinking Water Health Advisory for microcystin is 0.3 micrograms per liter (µg/L) for bottle-fed infants and pre-school children and 1.6 µg/L for school-age children and adults (EPA, 2015).

The World Health Organization (WHO) has developed a guideline for ingestion of microcystin-LR in drinking water. A provisional tolerable daily intake (TDI) of microcystin-LR has been set at 0.04 μg/kg body weight per day (WHO, 1999). Using this TDI, WHO developed the guideline value for lifetime consumption at 1.0 μg/L for a 60 kg adult with an average water intake of 2 liters per day.

WHO has also developed risk probability levels for exposure to microcystin-LR in recreational waters. These guidelines are divided into a mild/low, moderate, and high level of risk depending on algae bloom cell concentration. A relatively mild and/or low probability of adverse health effects from dermal exposure while using recreational waters was set for a bloom concentration of 20,000 cells per milliliter (cells/mL). This corresponds to an estimated microcystin concentration range of 2-4 μg/L. A moderate probability of adverse health effects from exposure to recreational waters was set for a bloom concentration of up to 100,000 cells/mL, corresponding to an estimated microcystin concentration of 20 μg/L. Finally, a high risk of adverse health effects from exposure to recreational waters was set for a bloom with concentrations greater than 100,000 cells/mL or with dense algae scum formation. This corresponds to a microcystin concentration range of 25 to 50 μg/L (WHO, 1999). The bloom concentrations of 20,000 and 100,000 algal cells/mL are important benchmarks and were used as two testing parameters during this research, as described in **Section 2.2.1.2**.

1.4 Current Treatment Options

1.4.1 Physical Separation
Coagulation, flocculation and, sedimentation have been conventional methods for the removal of suspended materials in drinking water for decades. However, the removal of algae cells by these traditional methods can have varying degrees of success due to algae's low specific gravity, surface charge, motility, and cell morphological properties (Ghernaout et al., 2010). It has also been found that these treatment techniques do not effectively remove the cyanotoxins produced by algae cells (He at al., 2016). The relatively large size of algae cells can facilitate effective removal of cells by rapid sand filtration (Borchardt & O'Melia, 1961). However, traditional sand and gravel filter media does not remove algal cyanotoxins from water and may also disrupt cell integrity as they accumulate on the filter media, causing the release of more toxins (He et al., 2016). Finally, dissolved air flotation (DAF) has been shown to effectively remove algae cells from suspension, especially when performed with chemical flocculation and solids recycle (Bare et al., 1975; Edzwald, 1993). This method does not effectively remove cyanotoxins produced by the algae and is more energy intensive and expensive than traditional methods.

1.4.2 Chemical Oxidation

Strong chemical oxidants including free chlorine (NaOCl), chlorine dioxide (ClO$_2$), monochloramine (NH$_2$Cl), and permanganate (KMnO$_4$), as well as advanced oxidation by ozone are current methods utilized at facilities treating source water containing harmful algal blooms (He et al., 2016). Oxidation with chlorine-based compounds may induce cell lysis, with research showing that doses of 3 to 6 mg/L of chlorine resulted in complete cell lysis (Daly et. al, 2007). As previously mentioned, oxidation of algal cells or toxins with chlorine oxidants may increase the formation of nitrogenous DBPs and release additional toxins into the water (Xie et al., 2013). Permanganate has successfully been used to inactivate algal cells and destroy cyanotoxins like microcystins (He et al., 2016); however, there is increasing concern with residual manganese concentrations in treated water. Manganese was placed on the EPA's Contaminant Candidate List (CCL4) in 2016 and a Secondary Drinking Water Standard of 0.05 mg/L has been set since. Finally, ozone has been shown to be one the most effective methods for oxidizing algae and other organics over chlorine-based chemicals (Wert et al., 2013); however, there is a high capital cost for installation of generation and treatment units for a system that would only be used during the short duration of bloom conditions.

1.5 Ferrate

Recently, ferrate (Fe(VI)) has been evaluated as an alternative oxidant for organic and inorganic contaminants in drinking water. The most commonly considered application of Fe(VI) in treatment is as a pre-oxidant, meaning it is applied before clarification. Potassium ferrate (K$_2$FeO$_4$) is a strong oxidant in both acidic and alkaline conditions with the standard electrode potential of 2.20 and 0.72 V, respectively (Lee et al., 2004). Fe(VI) has the advantage of forming species of ferric iron (Fe(III)) after it has been reduced, which could potentially aid in coagulation, flocculation, and sedimentation (Goodwill et al., 2016). Besides automatic decomposition, other oxidant demands such as natural organic matter, reduced metals, and pathogens may also react with Fe(VI). The common reaction pathways for Fe(VI) in water are shown in Figure 1 (Goodwill et al., 2016). As seen in the figure, there are multiple and complex pathways for Fe(VI) reactions in raw water.

As(III)—arsenite, As(V)—arsenate, DBPFP—disinfection by-product formation potential, DOC—dissolved organic carbon, EDCs—endocrine disrupting chemicals, Fe(II)—ferrous, Fe(III)$_{(s)}$—ferric solid, Mn(II)—manganous, Mn(IV)$_{(s)}$—manganese oxide solid, Mn(VII)—permanganate
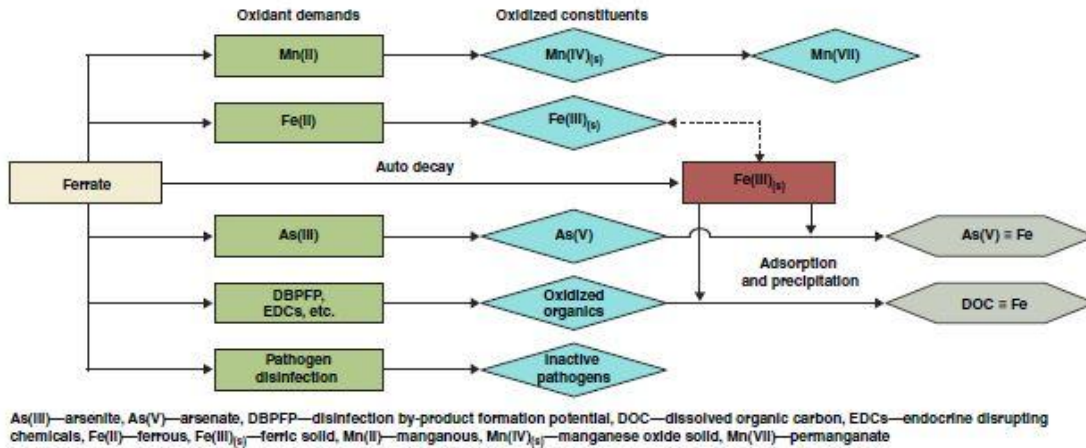
Figure 1: Common Pathways of Reaction for Fe(VI) in Drinking Water Treatment
(Image Source: Goodwill et al., 2016)

The performance of Fe(VI) as a pre-oxidant in drinking water treatment has been compared to other typical chemical oxidants like ozone and permanganate. Fe(VI) has been found to be comparable to ozone for the removal of halogenated DBP pre-cursors in natural waters and can provide lower yields of brominated DBPs formed with subsequent chlorination (Jiang et al., 2019). Fe(VI) pre-oxidation has not been found to have negative impacts on subsequent coagulation steps and has actually been found to improve finished water turbidity, UV$_{254}$ absorbance, and disinfection by-product formation as compared to permanganate (Goodwill et al., 2016).

A comparison of particulate characteristics on particles that were reduced by Fe(VI) versus those treated with ferric chloride showed that Fe(VI) oxidation produces significantly higher concentrations of nanoparticles and forms a stable suspension of negatively charged particles. Scanning electron microscopy (SEM) micrographs showed that the Fe(VI) reduced particles were smoother and had a more uniform surface morphology (Goodwill et al., 2015).

Currently, there is much literature available for the use of Fe(VI) in general water treatment; however, not much research has been conducted on its specific use as an oxidant for algae treatment. Preliminary research into its use for this purpose illustrated that inactivation of algae cells is possible with varying impacts to cell integrity and that some removal of inactivated cells occurred via enhanced coagulation by iron species (Zhou et. al, 2014). The proposed reactions between Fe(VI) and algal cells is presented in Figure 2, below. Coupling these new possible interactions between Fe(VI) and algae cells and associated organic matter along with reaction pathways proposed in Figure 1, it is clear that a complex system of interactions is possible during the addition of Fe(VI) in water.
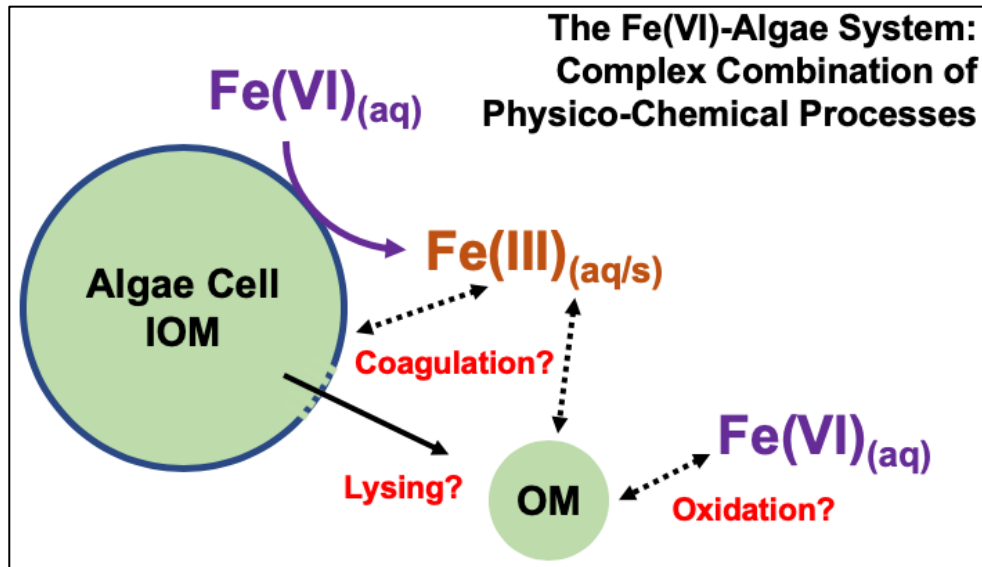
Figure 2: Proposed Interactions Between Fe(VI) and Algal Cells
(Image Source: Erika Addison – University of Rhode Island)

The effect of Fe(VI) oxidation on the cell integrity, release of intracellular organic matter (IOM), and the formation of disinfection by-products (DBPs) by *M. aeruginosa* has been studied with flow cytometry. It was found that significant cell lysis does not occur, regardless of the Fe(VI) dose, but that IOM release can increase with increasing Fe(VI) dose. Enhanced coagulation was performed in these experiments and was found to reduce the concentration of algal cells, decrease the algal organic matter, and reduce the formation of DBPs. However, this study was performed at an algae cell concentration of 1,000,000 cells per milliliter and does not accurately represent typical bloom conditions, as outlined by the World Health Organization (WHO) (Zhou et al., 2014).

Fe(VI) pre-oxidation on algae has been shown to enhance removal of algae cells by coagulation specifically with alum $(Al_2(SO_4)_3 \cdot 18H_2O)$ (Ma & Liu, 2002). The efficiency of algae removal by alum coagulation has also been found to be enhanced by increased pre-oxidation time. Pre-oxidation with Fe(VI) can also reduce the required dose of alum for efficient algae removal (Ma & Liu, 2002).

An increase in UV_{254} absorbance due to inactivated algae cells secreting intracellular and extracellular organic matter (IOM and EOM, respectively) has been observed in algae waters oxidized with Fe(VI). Through bridging mechanisms, this matter can act as a coagulant aid (Ma & Liu, 2002). However, this research was performed on the algae species *Scenedesmus* and *Chlorococoum* and results may vary for other algae species. Excitation emission matrix (EEM) spectra by fluorescence spectroscopy have been used to shown that oxidation with Fe(VI) alters intracellular dissolved organic matter (IDOM) and extracellular dissolved organic matter (EDOM) of *M. aeruginosa* (Liu et al., 2017). Fe(VI) doses as low as

15 µM (as Fe(VI)) can induce changes in humic and proteinaceous compounds within the algae cells (Liu et al., 2017). Oxidation by Fe(VI) has also been found to reduce concentrations of chlorophyll-a (Chl-a) in algae, which is used as a common indicator for cell vitality (Liu et al., 2017). Although these results are promising, experiments were performed on waters with a *M. aeruginosa* concentration of 10,000,000 cells/mL, which is significantly above the bloom conditions guidelines set by the World Health Organization (WHO).

Finally, Fe(VI) is capable of oxidizing the cyanotoxin, microcystin-LR, by second order kinetics; however, the reaction rate decreases with increasing pH values above 7.5 (Jiang et al., 2014). The products of microcystin oxidation, as measure by liquid chromatography-mass spectrometry/mass spectrometry (LC-MS/MS), were shown to form from the hydroxylation of the cyanotoxin aromatic ring. Additionally, ferrate oxidation caused fragmentation of the cyclic microcystin-LR structure, which produced by-products that did not possess significant biological toxicity (Jiang et al., 2014).

The objective of this study was to gain a better understanding of the impact Fe(VI) oxidation has on algae cells to provide more insight into its potential use as an intermittent treatment solution to reduce risks from HABs in drinking water sources.

Chapter 2: Methods

2.1 *Microcystis aeruginosa* Culturing

2.1.1 Source of Algae
Live algal strains of Culture Collection of Algae at the University of Texas at Austin (UTEX) UTEX LB 2386 *Microcystis aeruginosa* (*M. aeruginosa*) were obtained from the University of Texas on May 31, 2018. This strain of *M. aeruginosa* originated from Little Rideau Lake in Ontario, Canada and was collected in September 1954. Strains were received in Bold 3N growth media and were refrigerated until transferred to fresh Bold 3N growth media. Four cultures (150 milliliters (mL) each) were started from the original strains by transferring 10 mL of received algae stock to 140 mL of freshly prepared Bold 3N media in a 200 mL Erlenmeyer flask.

2.1.2 Culture Media
Cultures of *M. aeruginosa* were grown in laboratory prepared UTEX Bold 3N media for xenic cultures of freshwater blue-green and red algae. Growth media was prepared by adding approximately 850 mL of reagent grade water to a 1000 mL volumetric flask. The following reagents were then added in this specific order: 30 mL of 25 gram per liter (g/L) sodium nitrate solution ($NaNO_3$), 10 mL of 2.5 g/L calcium chloride dihydrate solution ($CaCl_2 \bullet 2H_2O$), 10 mL of 7.5 g/L magnesium sulfate heptahydrate solution ($MgSO_4 \bullet 7H_2O$), 10 mL of 7.5 g/L potassium phosphate dibasic solution (K_2HPO_4), 10 mL of 17.5 g/L potassium phosphate monobasic solution (KH_2PO_4), 10 mL of 2.5 g/L sodium chloride solution (NaCl), 6 mL of P-IV metal solution (described below), and 40 mL of UTEX Soilwater: GR+ Medium (purchased from UTEX). The Bold 3N media solution was brought to 1000 mL with reagent grade water and stored at 4°C until it was autoclaved prior to use. After the growth media was autoclaved and cooled to below 48°C, 1 mL of Vitamin B_{12} solution (described below) was added.

The P-IV metal solution was produced by first dissolving 0.75 grams of ethylenediaminetatraacetic acid disodium salt dihydrate ($Na_2EDTA \bullet 2H_2O$) in approximately 500 mL of reagent grade water in a 1000 mL volumetric flask. Once fully dissolved, the following were added: 97 milligrams (mg) of iron (III) chloride hexahydrate ($FeCl_3 \bullet 6H_2O$), 41 mg of manganese chloride tetrahydrate ($MnCl_2 \bullet 4H_2O$), 100 mL of 50 mg/L zinc chloride ($ZnCl_2$) solution, 100 mL of 20 mg/L cobalt (II) chloride hexahydrate ($CoCl_2 \bullet 6H_2O$) solution, and 100 mL of 40 mg/L sodium molybdate dihydrate ($NaMoO_4 \bullet 2H_2O$) solution. The P-IV metal solution was brought to 1000 mL with reagent grade water.

The Vitamin B_{12} solution was prepared by dissolving 2.4 grams of HEPES buffer in 200 mL of reagent grade water and adjusting the pH to 7.8 with 1 N NaOH. Next, 27 mg of Vitamin

B$_{12}$ was added to the solution. Finally, the solution was aseptically filtered through a 0.45 μm glass fiber filter. This method was used to sterilize the solution because autoclaving would degrade the Vitamin B$_{12}$. The solution was pipetted into pre-autoclaved 1 mL capped tubes and frozen until used in Bold 3N growth media.

2.1.3 Culture Propagation

Algae were grown in 200 mL Erlenmeyer flasks. Flasks were capped with a cotton ball and gauze plug to prevent introduction of foreign material into the culture but provide passage of air into the flask. Algae cultures were kept on a New Brunswick Scientific innOva 2000 platform shaker (New Brunswick Scientific Co., Inc., Edison, NJ) set at 100 revolutions per minute (rpm). Cultures were kept under an LED shoplight hung about eighteen inches from the top of culture flasks. A luminescence of 200 foot-candles was targeted for growth and a 16 hour "on" and 8 hour "off" timer was set for the shoplight.

Algae cultures were propagated every two weeks to continually provide algae samples within the logarithmic growth phase of their lifecycle. Each of the four cultures were designated as a series and labeled A through D with transfers occurring linearly by numeric series, as shown in Figure 3 (for the first three series).
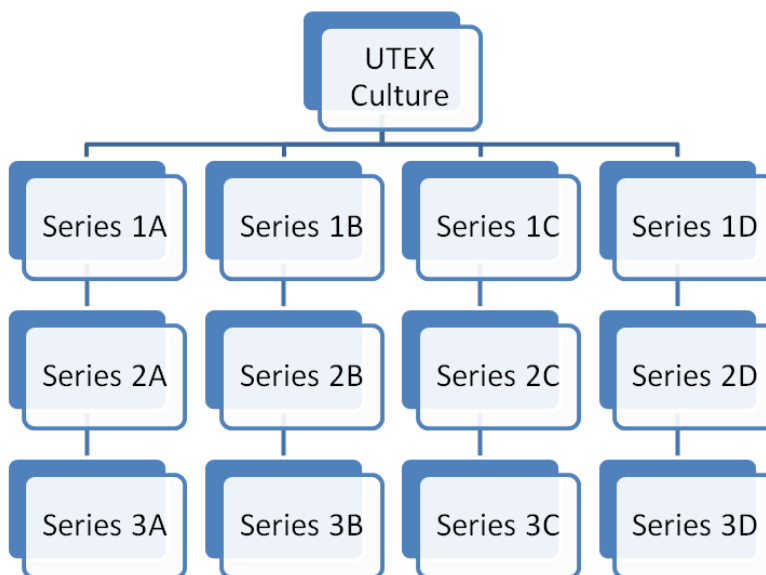
Figure 3: Algae Culture Transfers and Nomenclature

The particle count of the previous culture was determined on day fourteen of growth and was used to calculate the volume of culture that needed to be transferred to start the new 150 mL culture at 60,000 particle counts per milliliter (pc/mL). The following equation was used to calculate the volume of algae solution needed to be transferred to the new culture:

$$V_T = \frac{(150)(60{,}000)}{C_T} \qquad \text{(Equation 1)}$$

Where V_T was the volume of algae stock to be transferred (mL) and C_T was the particle count of the previous culture that was being used for the transfer (pc/mL). The new culture was brought to 150 mL by adding the appropriate volume of Bold 3N media.

Glassware and Bold 3N media (without Vitamin B_{12}) were autoclaved in a Market Forge Electric Sterilmatic Sterilizer (Market Forge Industries, Inc., Everett, MA) for 30 minutes at 121°C. Glassware and media were allowed to cool to below 48°C before Vitamin B_{12} was added to the growth media. Transfers were performed aseptically in a laminar flow hood to prevent contamination of specimen. All surfaces and equipment was disinfected with a 50 percent alcohol solution, prepared by diluting 95% HistoPrep™ RA alcohol (Fisher Healthcare, Pittsburg, PA) with reagent grade water at a one part to one part ratio, prior to use.

The distinct phases of culture growth are exemplified by Culture Series 8A, as depicted in Figure 4. The lag growth phase of culture growth typically lasted between 8 and 10 days after transfer. The logarithmic growth phase was typically between 10 and 22 days after transfer. The stagnation phase of culture growth typically started after 25 days and ultimately led to the death phase. A growth curve similar to that depicted in the figure was targeted for all algae cultures.
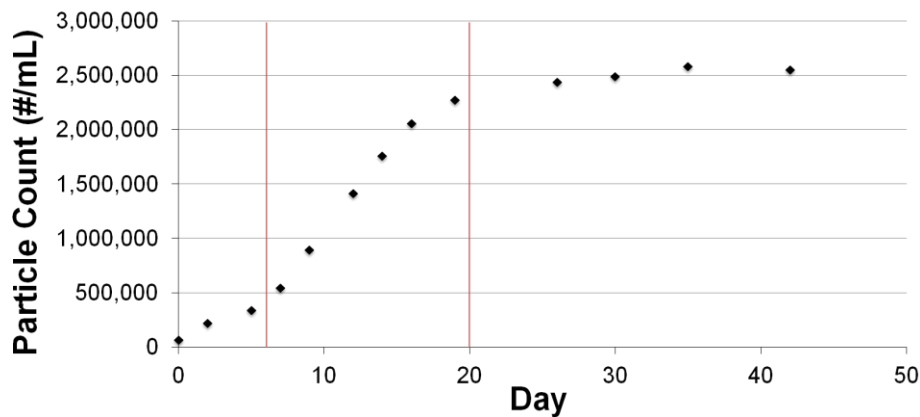
Figure 4: Typical Algae Culture Growth Curve (Culture Series 8A)

2.2 Experimental Design

Operating parameters and post-treatment analytical parameters were selected to determine the impact of ferrate oxidation on algal properties. This section describes the testing parameters that were varied during experiments, the production of raw water samples, and set-up of the bench scale experiments.

2.2.1 Testing Parameters

The focus of this research was to determine how algae are affected by ferrate oxidation and how different pH conditions, algal concentrations, and ferrate doses influence these impacts. The figure included in **Appendix A** depicts the testing conditions used for experiments.

2.2.1.1 pH

Experiments were performed at a pH of 6.2 and 7.5 to encompass the common pH range for coagulation in conventional water treatment. See **Section 2.2.2** for adjusting pH for raw water samples.

2.2.1.2 Algae Concentration

Raw water was prepared with either a low or high *M. aeruginosa* concentration (20,000 or 100,000 particle counts (pc)/mL, respectively). World Health Organization guidelines were used to determine the two algae concentrations for experimentation (WHO, 1999). A low algae concentration of 20,000 pc/mL correlates to a relatively low probability of adverse health effects while a high algae concentration of 100,000 pc/mL correlates to a moderate probability of adverse health effects due to the potential concentration of microcystin-LR present. See **Section 2.2.2** for details on algae concentration in the production of raw water.

2.2.1.3 Ferrate Dose

Potassium ferrate (K_2FeO_4) was obtained from Element 26 Technology (Friendswood, TX). The purity of the potassium ferrate was determined to be approximately 88%. Solid potassium ferrate was kept wrapped in aluminum foil and in a moisture free desiccator to prevent hydrolysis and degradation. Periodically, the purity of solid potassium ferrate was tested by comparing the actual direct absorbance of a potassium ferrate stock solution of known concentration (assuming 100% chemical purity) at 510 nm to the expected theoretical absorbance for that concentration. The following equation was used to determine the purity of the potassium ferrate chemical.

$$Purity = \frac{A_a}{A_T} \times 100\% \qquad \text{(Equation 2)}$$

Where A_a is the actual measured absorbance of the solution at 510 nm and A_T was the theoretical absorbance determined by the following equation.

$$A_T = [Fe(VI)] x \, \varepsilon \, x \, l \qquad \text{(Equation 3)}$$

Where [Fe(VI)] is the concentration of potassium ferrate stock solution (moles/L), ε is a constant (assumed as 1150 $M^{-1}cm^{-1}$ (Lee et al., 2005)), and l is the path length (1 cm).

The purity of chemical was used to adjust appropriate mass of potassium ferrate used for dosing experiments. Potassium ferrate chemical with an 80% or higher purity was used for experiments.

Ferrate doses of 20 µM, 50 µM, and 100 µM (as ferrate) were used during experiments. The amount of potassium ferrate used for dosing was determined with the following equation:

$$Mass\ K_2FeO_4\ (mg) = \left[\frac{\left(\frac{C}{8.34} \times \frac{198.843}{119.845} \right)}{Purity} \right] \times V_s \qquad \text{(Equation 4)}$$

Where C is the target concentration of ferrate (µM), purity is the purity as determined above, and Vs is the volume of sample to be treated (0.8 L for these experiments). Molecular weights of 119.843 grams per mole (g/mol) and 55.845 g/mol were used for FeO_4^{2-} (Fe(VI)) and Fe, respectively. A molecular weight of 198.843 g/mol was used for K_2FeO_4. The conversion factor 8.34 mol/mg was the ratio of 1 mole Fe(VI) to 119.9 grams Fe(VI).

The actual dose of ferrate was determined using the total iron concentration, as described in **Section 2.3.5**.

2.2.2 Production of Raw Water

Raw water samples were prepared in the laboratory on the day of testing by adding a volume of algae stock solution to reagent grade water followed by buffering and pH adjustment. To separate algae cells from the growth media, a 30 mL sample of algae was taken from a culture within the logarithmic phase of growth (typically at 15 to 22 days of growth) and aseptically transferred to a 50 mL Nalgene™ Oak Ridge High-Speed centrifuge tube with screw cap (Fisher Scientific, Pittsburg, PA). The algae stock was centrifuged at 3,000g and 4°C for 10 minutes on a Fisher Scientific Marathon 21000R refrigerated centrifuge (Fisher Scientific, Pittsburg, PA) with a swing bucket rotor. Supernatant was poured off and the algae pellet remaining in the centrifuge tube was resuspended in 30 mL of reagent grade water. Samples were shaken until the algae pellet was well mixed before inserting into the centrifuge for a second 10 minute cycle at 3,000g and 4°C. Supernatant was poured off and the algae pellet remaining was resuspended for a second time in 30 mL of reagent grade water to form the algae stock solution used for raw water dosing. The particle count of the algae stock solution was then measured. The volume of algae stock added to raw water samples was determined using the following equation:

$$V_s = \frac{P_w V_w}{P_s} \qquad \text{(Equation 5)}$$

Where V_s was the volume of algae stock required (mL), P_w was the particle count desired in the raw water sample (pc/mL), V_w was the volume of the raw water sample (mL), and P_s was the particle count of the algae stock (pc/mL). The particle count of the resulting raw water was determined on the Chemtrac PC 5000 (Chemtrac, Inc., Norcross, GA). The particle count was further adjusted by dilution or addition of algae stock determined by Equation 5 if the raw water particle count was not within 7,000 pc/mL for the low algae concentration (20,000 pc/mL) or within 10,000 pc/mL for the high algae concentration (100,000 pc/mL).

After achieving the desired algae count, the water was buffered. The bicarbonate buffer was prepared by filling a 500 mL volumetric flask approximately halfway with reagent grade water and dissolving 21.0 grams of sodium bicarbonate ($NaHCO_3$) into solution. The solution was brought to the mark with reagent grade water and then the pH was adjusted to 7.5 with 6 N HCl. 2 mL of 0.5 M bicarbonate buffer (pH=7.5) was added to the raw water to achieve a final buffer concentration of 1 mM. Lastly, the pH was adjusted to 6.2 or 7.5 with 0.05 M NaOH or 1 N HCl, as needed.

2.2.3 Bench-scale Set-up

Once raw water was prepared, the appropriate mass of potassium ferrate (K_2FeO_4), as described in **Section 2.2.1.3**, was weighed on an analytical balance. Raw water was placed on a magnetic stir plate set at 150 rpm to simulate a rapid mixing phase. A 200 mL sample was taken for pre-treatment analysis. Using a small amount of reagent grade water, the potassium ferrate was added to the raw water and a stopwatch was started. At designated time intervals 9.5 mL samples were taken for ferrate concentration measurement. At 1 minute of treatment time, mixing was reduced to approximately 80 rpm to simulate a slow mixing phase. At the appropriate reaction time, a 200 mL sample was taken for post-treatment analysis.

Reaction times varied for each testing condition. The ferrate-algae reaction for each experiment was considered at completion when the change in measured ferrate concentration in post-treatment water samples was below 5 percent. For experiments at pH 6.2, reactions were generally complete after 15 minutes of reaction time. For experiments at pH 7.5, 25 minutes of reaction time was typically required before changes in ferrate concentration were less than 5 percent. Some dosing conditions at pH 7.5 required up to 30 minutes of reaction time to reach completion. It is important to note that no ferrate quenching agent was introduced to post-treatment samples, which allowed continued reaction time while grab samples were being prepared for analytical testing.

2.3 Analytical Procedures

The physical and chemical water quality analyses that were performed in the laboratory on pre-treatment and post-treatment water samples are summarized in Table 1.

Table 1: Sample Analyses Information

Parameter	Pre-treatment/Post-treatment	Method	Instrumentation
pH	Both	SM 4500 – H$^+$ B	Orion 720 pH Meter
Particle Counts	Both	SM 2560 C	Chemtrac PC 5000
UV$_{254}$	Both	SM 5910 B	HACH DR6000 Spectrophotometer
Organic Carbon • TOC • DOC	Both Both	SM 5310 B	Shimadzu TOC-5000A Analyzer
Total Iron • 0.7µm Filter • 0.22µm Filter • 30kDa Filter	Both Post-treatment Post-treatment Post-treatment	SM 3500-Fe D	HACH DR6000 Spectrophotometer
Total Nitrogen	Both	SM 4500-N$_{org}$ D EPA 353.2	LACHAT QuikChem 8500-Series 2 Flow Injection Analyzer
Ferrate Decay	Post-treatment	ABTS (Lee et al.)	HACH DR6000 Spectrophotometer

Notes: SM = Standard Methods for the Examination of Water and Wastewater;
EPA = United States Environmental Protection Agency

2.3.1 pH

An Orion 720 pH probe (Thermo Electron Corporation, Waltham, MA) with an Accumet AB15 Benchtop pH Meter (Fisher Scientific, Pittsburg, PA) was used to measure pH in the laboratory in accordance with Standard Method 4500 – H$^+$ B (APHA et al., 2017). The pH meter was calibrated weekly with the use of Fisher Scientific pH 4, 7, and 10 buffers (Fisher Scientific, Pittsburg, PA). The pH of raw water was adjusted according to **Section 2.2.2** and recorded. The pH of post-treatment water was monitored continuously for the duration of the reaction time and continuously adjusted to the appropriate pH value using 0.05 M NaOH or 1N HCl.

2.3.2 Particle Count

A Chemtrac PC5000 (Chemtrac, Inc., Norcross, GA) particle counter was used to determine total particle counts and size distribution of particles by Standard Method 2560 C (APHA et al., 2017). Eight size range categories were set during sample analysis. They included 2-3 µm, 3-6 µm, 6-9 µm, 9-16 µm, 16-27 µm, 27-44 µm, 44-75 µm, 75-125 µm. The ninth size range is automatically set by the PC5000 depending on upper limit of the eighth size range. This last range included particles greater than 125 µm. Due to the PC5000 having a maximum coincidence level of 20,000 counts per milliliter, samples were diluted prior to analysis by adding 1 mL of sample water to a 100 mL volumetric flask and filling to the mark with reagent grade water. The PC5000 was set to a 75 mL per minute (mL/min) flow rate, a 30 mL purge volume, a 25 mL sample draw volume, and duplicate readings per sample. A graduated cylinder and stopwatch was used to confirm the flow rate of 75 mL/min before and after samples were analyzed. To prevent residual particles from being transferred between samples, approximately 100 mL of reagent grade water was passed

through the PC5000 instrument before and after samples were analyzed. Particle counts for a 100 mL sample of the same reagent grade water used for sample dilution was determined before and after samples were analyzed. The average particle count of the dilution water and the average diluted sample particle count were used to determine the actual particle count of samples by the following equation:

$$P = \frac{(C_a \times 100 \; mL) - (C_w \times 99 \; mL)}{1 \; mL} \qquad \text{(Equation 6)}$$

Where P is the actual undiluted particle count (pc/mL), C_a is the average diluted particle count read from the PC5000 (pc/mL), and C_w is the average reagent grade water particle count read from the PC5000 (pc/mL).

2.3.3 Total and Dissolved Organic Carbon

Total organic carbon (TOC) and dissolved organic carbon (DOC) were measured using a Shimadzu TOC-5000A analyzer (Shimadzu Corporation, Kyoto, Japan). Samples were prepared, stored, and analyzed with a method adapted from Standard Method 5310 B (APHA et al., 2017). Glassware used for TOC/DOC analysis was acid bath washed in a 20 percent sulfuric acid bath for a minimum of one hour and then triple washed with reagent grade water. Samples of pre-treatment and post-treatment water were analyzed in duplicate and results were averaged. Approximately 10 mL, each, of pre-treatment and post-treatment samples were transferred into three acid-washed vials for TOC analysis. Approximately 10 mL, each, of pre-treatment and post-treatment samples were filtered through 25 mm diameter Whatman glass fiber filters (GF/C) with a 1.2 μm pore size (Whatman Inc., Clifton, NJ) into three acid-washed vials for DOC analysis. Filters were prewashed with approximately 30 mL of reagent grade water prior to use. All samples were acidified to a pH of 2 with 3N H_2SO_4 by using a 1 μL acid to 1 mL sample ratio. DOC samples were tested for UV_{254} absorbance (see **Section 2.3.4**) prior to being acidified.

To limit exposure of samples containing algae to acid, a calibration curve was run and stored on the instrument prior to any TOC/DOC sample analysis. Samples were run in the following order to limit acid exposure to less than one hour; 1) duplicates of pre-treatment TOC, 2) duplicates of pre-treatment DOC, 3) duplicates of post-treatment TOC, and 4) duplicates of post-treatment DOC. Acidified samples were capped with parafilm and plastic Shimadzu caps (Shimadzu Corporation, Kyoto, Japan). Samples were not stored overnight.

The Shimadzu TOC-5000A was calibrated with a three-point potassium hydrogen phthalate calibration curve (0, 2, and 4 mg/L TOC) prior to analysis. The calibration standards were prepared by preparing a 1000 mg/L primary potassium hydrogen phthalate stock standard. This stock standard was prepared by first drying 0.75 grams of potassium hydrogen phthalate in an oven at 105°C for approximately 30 minutes, then cooling for approximately 20 minutes. Once cooled, 0.5314 grams of the dried potassium hydrogen

phthalate was added to an acid-washed 250 mL volumetric flask, which was then filled to the mark with reagent grade water. The resulting 1000 mg/L stock solution was stored in an amber glass bottle at 4°C for up to three weeks.

A 100 mg/L intermediate potassium hydrogen phthalate stock standard was created by diluting the 1000 mg/L primary stock. 10 mL of the primary stock was transferred to an acid-washed 100 mL volumetric flask and diluted to the mark with reagent grade water. The 100 mg/L intermediate stock solution was used to prepare the working standards of 0, 2, and 4 mg/L. The working standards were prepared by filling acid-washed 100 mL volumetric flasks approximately halfway with reagent grade water, transferring the appropriate amount of intermediate stock (e.g. 4 mL for the 4 mg/L working stock), acidifying with 100 μL of 3N H_2SO_4, and filling to the mark with reagent grade water. For quality control, a calibration standard with known concentration was analyzed as a sample during sets of sample analysis.

Samples were sparged for five minutes with ultra-zero air before analysis to remove any carbon dioxide. The standards and samples were analyzed a minimum of three times to provide a standard deviation and coefficient of variation less than 200 or 2.0 percent, respectively. If these values were exceeded, up to two additional readings would be taken per sample, with three readings that met the criteria used to determine the organic carbon concentration. The calibration curve was created using peak areas from the prepared standards and sample concentrations in mg/L were measured based on the calibration curve.

2.3.4 UV$_{254}$ Absorbance

Pre-treatment and post-treatment samples were analyzed for UV_{254} absorbance in accordance with Standard Method 5910 B (APHA et al., 2017). As described in **Section 2.3.3**, samples prepared for DOC analysis were filtered through a 25 mm diameter Whatman glass fiber filter (GF/C) with a 1.2 μm pore size (Whatman Inc., Clifton, NJ) and were analyzed for UV_{254} absorbance prior to being acidified. Samples were poured into a 1 cm quartz glass cuvette and UV_{254} absorbance measured on a HACH DR6000 spectrophotometer (HACH Company, Loveland, CO) using Program 411 for Organic UV_{254}. This method measures absorbance at 254 nm. Samples were analyzed in triplicate and averaged.

2.3.5 Total Iron and Iron Fractionation

Total iron and iron fractionation were measured using a 10 mL glass cuvette and Program 265 Iron FerroVer on the HACH DR 6000 spectrophotometer (HACH Company, Loveland, CO). HACH FerroVer Method 8008 for Total Iron, which is an adaptation to Standard Method 3500-Fe D Phenanthroline Method (APHA et al., 2017), was used for measurements. Iron fractionation was performed by filtering samples through a series of

filters with decreasing pore size. Filter cartridges, filter assemblies, and syringes were prewashed with reagent grade water and filters were washed with approximately 30 mL of reagent grade water prior to sample filtering. Samples were first filtered with a 25 mm diameter Whatman glass fiber syringe filter with a pore size of 0.7 μm and filtrate was tested for total iron. Samples were then filtered with a 47 mm diameter Durapore Membrane filter with a 0.22 μm pore size. Filtrate was tested for total iron. Finally, samples were filtered through a 44.5 mm diameter Millipore Ultracel® Ultrafiltration Disc ultrafilter (MilliporeSigma, Burlington, MA) with a 30 kilodalton (kDa) pore size using 50 psi of Nitrogen gas to drive water through the ultrafilter membrane. Filtrate was then analyzed for total iron.

Iron fractionation was determined using the total iron results after the series of filtering. Large particulate iron (C_1) was determined by subtracting the total iron in the filtrate of the 0.7 μm filter from the unfiltered total iron. Small particulate iron (C_2) was determined by subtracting the total iron in filtrate of the 0.22 μm filter from the total iron in the filtrate of the 0.7 μm filter. Colloidal iron (C_3) was calculated by subtracting the total iron in filtrate from the ultrafilter from the total iron in filtrate from the 0.22 μm filter. Dissolved iron (C_4) was simply the total iron in the filtrate of the ultrafilter.

Total iron samples were taken from pre-treatment water and at approximately 15 minutes of reaction time. The total iron concentration in the post-treatment samples was used to determine the actual ferrate dose introduced to the raw water sample. Although ferrate decays naturally in water, this method accounts for the total iron present in the sample and can therefore be used to back calculate the initial ferrate concentration. The following equation was used to calculate the starting ferrate dose from the total iron results:

$$[Fe(VI)] = 8.34 \times C \times \left(\frac{119.843}{55.845}\right) \qquad \text{(Equation 7)}$$

Where C was the total iron concentration (mg/L) contained in the sample at 15 minutes reaction time. Molecular weights of 119.843 grams per mole (g/mol) and 55.845 g/mol were used for FeO_4^{2-} (Fe(VI)) and Fe, respectively.

2.3.6 Ferrate Decay

Ferrate concentration was measured at set time intervals during treatment using a method developed by Lee, Yoon, and Gunten in which ferrate is reacted with 2,2'-azino-bis(3-ethylbenzothiazoline-6-sulfonate) (ABTS) to form a green radical cation (ABTS•+) that can be measured spectrophotometrically at 415 nanometers (Lee et al., 2005). Samples were analyzed using a HACH DR6000 spectrophotometer (HACH Company, Loveland, CO) set at a single wavelength of 415 nm.

Clean 25 mL glass vials were used to collect samples for ferrate analysis. Vials were labeled for each of the set time intervals of 0, 0.5, 1, 1.5, 2, 3, 5, 7, 10, 15, 20, 30, and 45 minutes. A volume of 2.5 mL of acetate/phosphate buffer and 0.5 mL ABTS stock solution was added to each vial. A 9.5 mL sample of pre-treatment water was added to the 0 minute vial, to act as the blank for the HACH DR6000 spectrophotometer. A 9.5 mL sample of post-treatment water was taken at each designated time interval and added to the appropriate vial. Reacted ferrate-ABTS solutions were stable for up to an hour and were analyzed for absorbance at 415 nm within this time. A 1 cm quartz glass cuvette was used to analyze samples. Absorbance data from the ABTS test was converted to concentration of ferrate (μM) with the following equation:

$$[Fe(VI)](\mu M) = \frac{A_{(415nm)} \times V_{final}}{\varepsilon \times l \times V_{sample}} \times 10^6 \qquad \text{(Equation 8)}$$

Where A is the absorbance taken at 415 nm wavelength, V_{final} is the final solution volume including the sample and reagents (12.5 mL), ε is a constant set at 34000 $M^{-1}cm^{-1}$(Lee et al., 2005), l is the path length (1 cm), and V_{sample} is the volume of sample in test solution (9.5 mL).

A 200 mL stock solution of 1 gram per liter (g/L) ABTS reagent was prepared by filling a 200 mL volumetric flask approximately halfway with reagent grade water and adding 0.2 grams diammonium-ABTS salt. This solution was mixed with a stir bar and mixing plate until the salt was dissolved. The solution was filled to the mark with reagent grade water, transferred to a glass bottle, and stored at 4°C for up to one month.

A 500 mL stock solution of 0.6 M Acetate/0.2 M phosphate buffer was prepared by filling a 500 mL volumetric flask approximately halfway with reagent grade water and 17.15 mL of acetic acid (CH_3COOH). 3.45 grams of sodium phosphate monobasic monohydrate ($NaH_2PO_4 \bullet H_2O$) and 13.35 grams of disodium phosphate dihydrate ($Na_2HPO_4 \bullet H_2O$) were dissolved into the solution. The solution was filled to the mark with reagent grade water and inverted to mix. This buffer solution was transferred to a glass bottle and stored at 4°C.

As a comparison to experiments conducted by Jiang et al. (2015), a second set of experiments were performed to specifically compare the decomposition rate of Fe(VI) in the presence of algae. Results from Jiang et al. are discussed in **Section 1.5**. To stay consistent with this previous work, experiments were conducted at pH 7.5, a Fe(VI) dose of 50 μM, and a bicarbonate buffer concentration of 2 mM. This was double the bicarbonate buffer concentration used for all other experiments. Algae concentrations of 0, 20,000, and 100,000 pc/mL were used in this set of tests. Reagents were prepared and samples were obtained and analyzed according to the procedure described above.

2.3.7 Total Nitrogen

Total nitrogen was measured on a Total Nitrogen manifold on a LACHAT QuikChem 8500-Series 2 Flow Injection Analyzer (LACHAT Instruments, Loveland, CO) using LACHAT QuikChem Method 10-107-04-4-B. This method was modified from Standard Method 4500-N_{org} D (APHA et al., 2017) and EPA Methods for Chemical Analysis of Water and Wastes Method 353.2 (EPA, 1993). For this method, 20 mL of pre-treatment or post-treatment sample was added to a 50 mL test tube with phenolic rubber lined screw caps and 5.0 mL of the basic potassium persulfate digestion reagent. Test tubes were prewashed in 1 M HCl solution and then triple washed in reagent grade water. 20 mL of 0, 0.1, 0.25, and 2.5 mg/L-N calibration standards and 20 mL of the 2.5 mg/L-N urea digestion check solution were also each added to test tubes with 5 mL of the basic potassium persulfate digestion reagent. Samples, calibration standards, and digestion check solutions were digested in a LACHAT BD40^{HT} (LACHAT Instruments, Loveland, CO) digester at 150°C for 30 minutes. Test tubes were allowed to cool to room temperature and then 0.5 mL of the acidic potassium persulfate digestion reagent was added to each test tube. Samples, calibration standards, and digestion check solutions were digested for a second time at 150°C for 30 minutes. Test tubes were allowed to cool to room temperature before analysis on the LACHAT QuikChem 8500. All water samples were digested in duplicates.

Digested samples, calibration standards, and digestion check solutions were inserted in the LACHAT ASX-560 Series XYZ AutoSampler. Reagent grade water was pumped through the Total Nitrogen manifold for 5 minutes before reaction reagents were introduced to the manifold flow lines. The reaction reagents were introduced in the following order: ammonium chloride buffer (pH 8.5), 0.5 N sodium hydroxide, 0.231 M sulfuric acid carrier, and sulfanilamide color reagent. Once all reaction reagents were introduced to the manifold, the flow line for the cadmium column was opened and flow was allowed to continue for 2 minutes prior to samples being analyzed. The calibration curve was created using peak areas from the prepared calibration standards and sample concentrations in mg/L-N were measured based on the calibration curve. Waste generated during this test was collected as hazardous waste.

50 mL of calibration standards were prepared by diluting a HACH 100 mg/L as NO_3-N Nitrate Nitrogen Standard Solution (HACH Company, Loveland, CO) to 0, 0.1, 0.25, and 2.5 mg/L. 50 mL of 2.5 mg/L-N urea digestion check solution was prepared by first preparing a 1000 mg/L-N stock urea solution and diluting it to 2.5 mg/L-N. The 1000 mg/L-N urea solution was prepared by dissolving 1.072 grams of urea (H_2NCONH_2) in 500 mL reagent grade water.

The following reaction reagents were prepared for use during this method:

A 500 mL solution of ammonium chloride buffer (at pH 8.5) was prepared by dissolving 42.5 grams ammonium chloride (NH_4Cl) and 0.5 g disodium ethylenediamine tetraacetic acid dihydrate ($Na_2EDTA \bullet 2H_2O$) in about 300 mL of DI water in a 500 mL volumetric flask. The solution was diluted to the mark and inverted to mix. The pH was adjusted to 8.5 with a 15 N NaOH solution.

A 250 mL solution of sulfanilamide color reagent was prepared monthly by adding 25 mL of 85% phosphoric acid (H_3PO_4) to approximately 150 mL of reagent grade water in a 250 mL volumetric flask. 10 grams of sulfanilamide and 0.25 grams of N-(1-napthyl)ethylenediamine dihydrochloride (NED) were then added. The solution was inverted to mix and then stirred with a stir bar and stir plate for 30 minutes. The solution was diluted to the mark, inverted to mix, and stored in an amber glass bottle. This solution was stable for one month.

The carrier for this test was a 0.231 M sulfuric acid solution. 8.4 mL of 11 N sulfuric acid was added to a 200 mL volumetric flask and then diluted to the mark with reagent grade water. This solution was prepared weekly.

A 500 mL solution of 0.5 N sodium hydroxide was prepared by dissolving 10 grams of NaOH in approximately 300 mL of reagent grade water in a 500 mL volumetric flask. The solution was diluted to the mark with reagent grade water and allowed to cool to room temperature before storing in a plastic bottle.

There were two digestion reagents for this test, a basic digestion reagent and an acidic reagent. 200 mL of the basic digestion reagent was prepared monthly by dissolving 2.1 grams of NaOH and 8.4 grams of potassium persulfate ($K_2S_2O_8$) in approximately 180 mL of reagent grade water in a 200 mL volumetric flask. The solution was diluted to the mark with reagent grade water and stored in a plastic bottle. 50 mL of the acidic digestion reagent was prepared by dissolving 1.15 grams potassium persulfate ($K_2S_2O_8$) in 30 mL of 11 N sulfuric acid in a 50 mL volumetric flask. The solution was diluted to the mark with 11 N sulfuric acid and inverted to mix. This solution was prepared weekly. It is important to note that potassium persulfate used for both of these reagents was nitrogen free.

Chapter 3: Results and Discussion

This chapter summarizes the results of ferrate oxidation treatment on laboratory prepared algae water, including data on particle counts, UV254 absorbance, total organic carbon and dissolved organic carbon, total iron and iron fractionation, ferrate decay, and total nitrogen. A discussion on the impacts of pH, algae concentration, and ferrate dose on post-treatment results follows.

3.1 Parameter Results

3.1.1 Particle Counts

Total particle counts of water samples were taken before and after treatment with potassium ferrate. Figure 5 shows the percent reduction after treatment for various pH conditions, Fe(VI) dose, and algae concentrations. The data illustrate that a reduction in total particle counts was observed in all samples after Fe(VI) treatment. As seen in the figure, greater percent reductions were generally achieved for waters with higher starting particle counts and for waters at pH 6.2. Particle counts were not significantly changed for waters at pH 7.5 treated with a 20 µM ferrate dose (reduction at both high and low algae was below 17%).
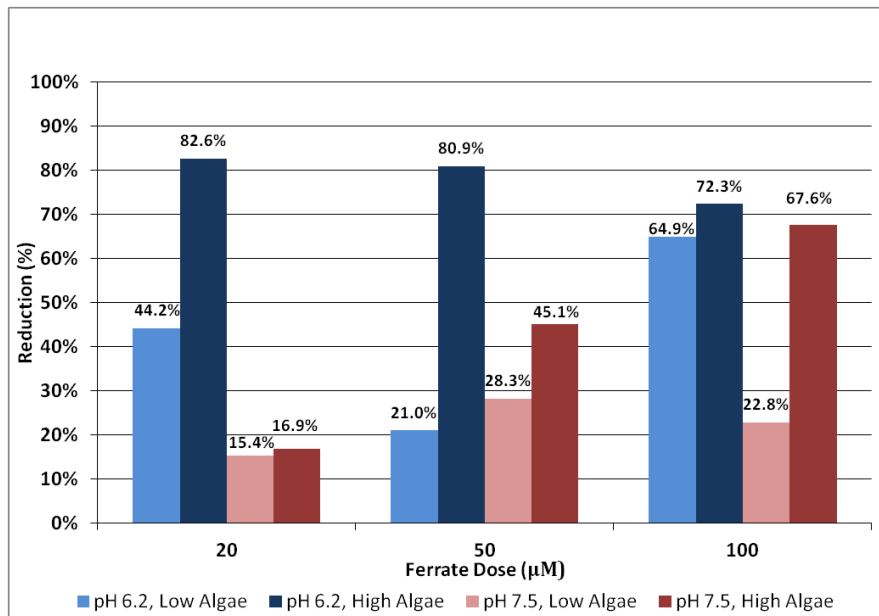
Figure 5: Average Reduction of Total Particle Counts

Figure 6 shows the average reduction of total particle counts at a pH of 6.2. As seen in the figure, the greatest reduction in particle counts for water with low algae (20,000 particle counts per milliliter (pc/mL)) occurred with a Fe(VI) dose of 100 µM, resulting in a 64.9% particle count decrease. For water with high algae (100,000 pc/mL), the greatest reduction

21

(82.6%) occurred with a 20 μM dose. The 20 μM dose at pH 6.2 and high algae resulted in the greatest observed particle count reduction in all samples. It is also noted that particle count reductions were generally high (72-83%) for all samples with 100,000 pc/mL algae. High percent reductions in total particle counts could indicate that some coagulation processes are occurring in post-treatment samples.
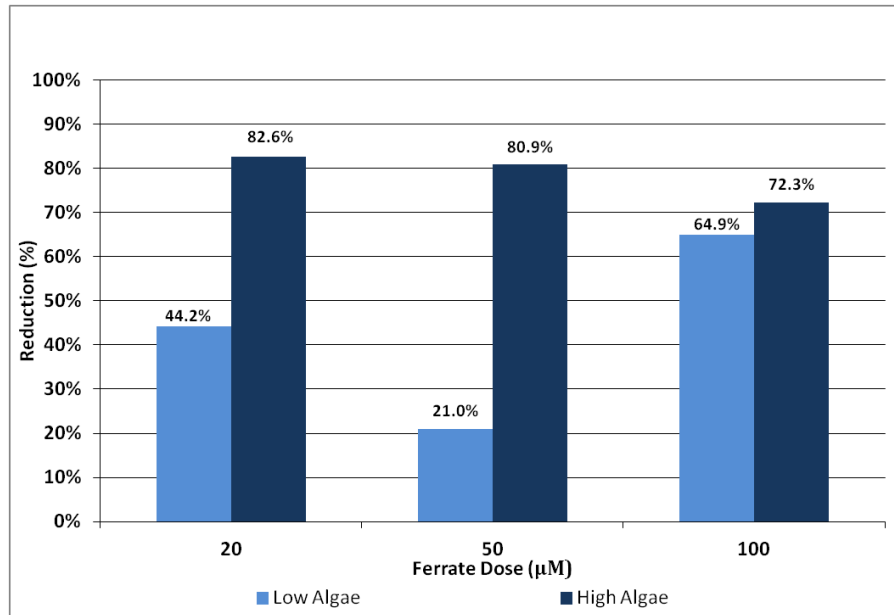
Figure 6: Average Reduction of Total Particle Counts (pH 6.2)

Figure 7 shows the average reduction of total particle counts at a pH of 7.5. As seen in this figure, the 50 μM ferrate dose produced the highest average percent particle count reduction for water with low algae (28.3%) and the 100 μM ferrate dose resulted in the highest percent particle count reduction for water with high algae (67.6%). Again, particle count reductions were greater on a percentage basis for samples with a high starting concentration.
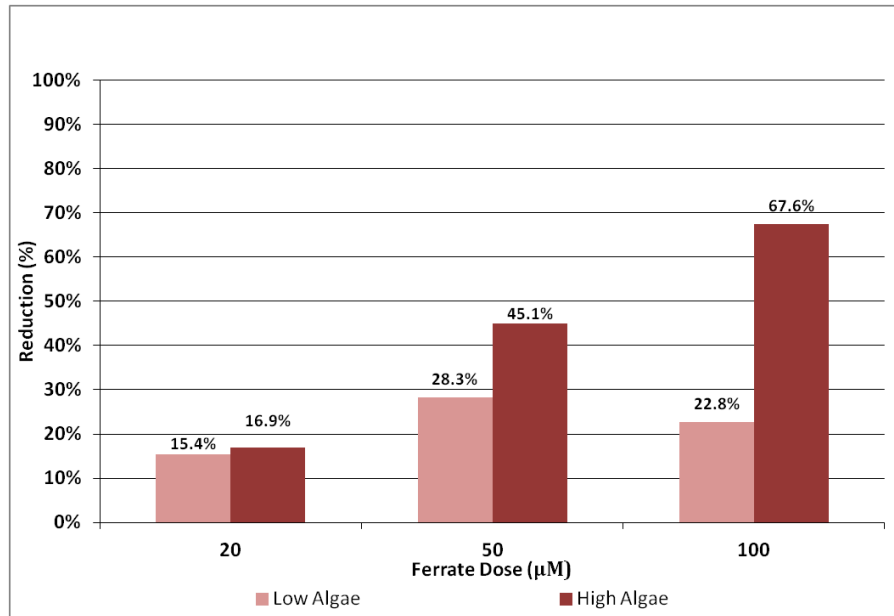
Figure 7: Average Reduction of Total Particle Counts (pH 7.5)

The change in particle size distribution was also analyzed before and after treatment with potassium ferrate. This analysis was performed by comparing particle counts in the first size range of the PC5000 (2-3 μm) to particle counts in all of the larger size ranges. It was found that the majority of particles in pre-treatment samples had sizes in the first size category of the PC5000 (2-3 μm), regardless of pH or algae concentration. The percent of particles in the 2-3 μm size category ranged from 72% to 95% of the total pre-treatment particle counts. Post-treatment samples were found to have fewer particles in the 2-3 μm size category than pre-treatment samples. The percent of particles in the 2-3 μm size category ranged from 45% to 81% of the post-treatment particle counts. This is exemplified in Figure 8, which shows the pre- and post-treatment particle size distribution for Experiment 5D. This test was conducted at a pH of 6.2, an algae concentration of 20,000 pc/mL, and a Fe(VI) dose of 20 μM.
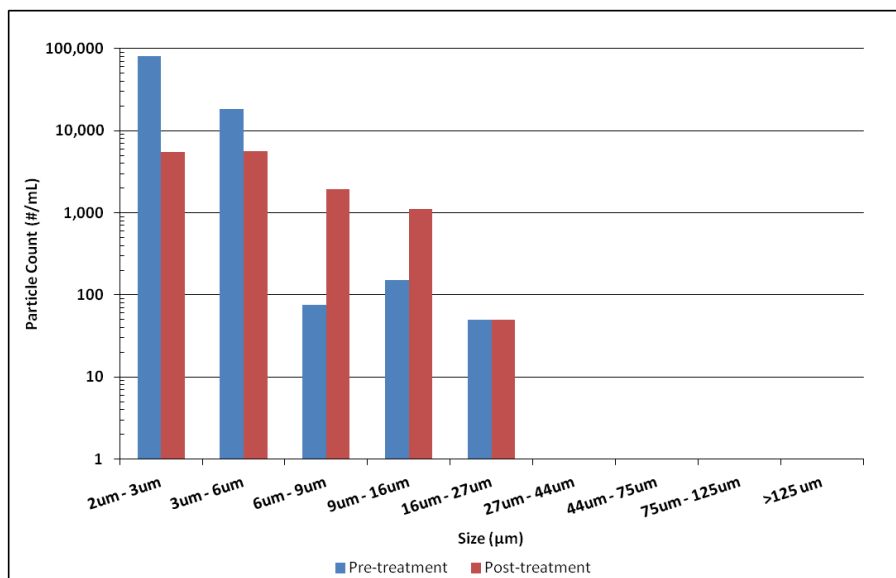
Figure 8: Example Particle Size Distribution

As seen in the figure, there were approximately 80,500 pc/mL in the 2-3 μm in the pre-treatment sample. This was decreased to approximately 5,600 pc/mL in the post-treatment sample. Meanwhile, the 6-9 μm and 9-16 μm size categories had increased counts in the post-treatment sample. A similar trend was observed under all conditions, with the majority of particles shifting from the first size category into the larger size categories after treatment with Fe(VI). Figure 9 and Figure 10 show the percent of total particle counts that were present in all of the size categories besides the 2-3 μm category (indicated as "large" particles), for each treatment condition. As seen in these figures, an increase in the percent of large particles was observed in post-treatment samples under all treatment conditions.
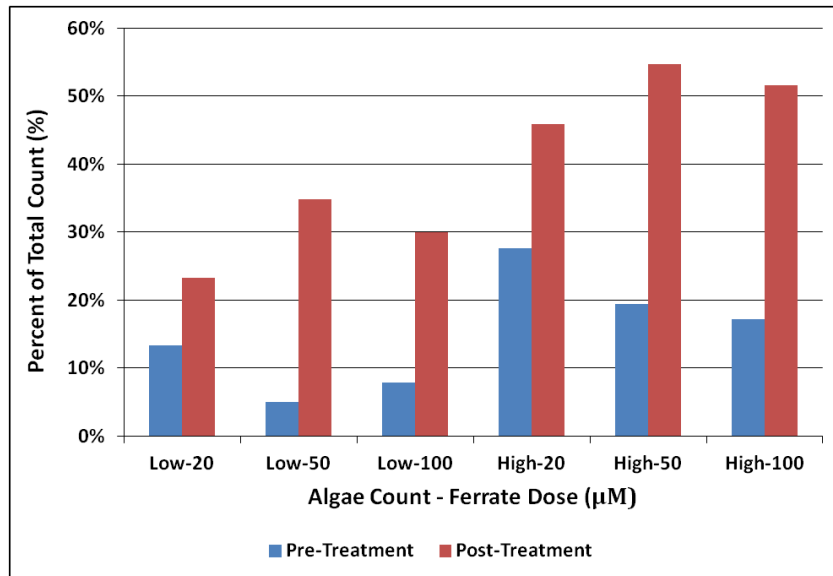
Figure 9: Percent of Total Particle Counts as Large Particles (pH 6.2)
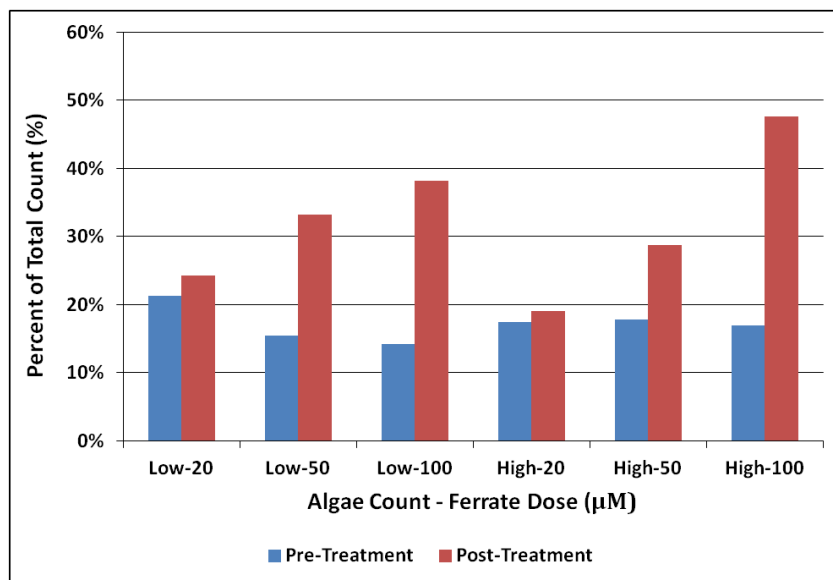
Figure 10: Percent of Total Particle Counts as Large Particles (pH 7.5)

As seen in Figure 9, the highest percentages of large particles were observed in post-treatment samples with pH 6.2 and a high algae concentration. Both the 50 μM and 100 μM doses resulted in more than 50% of post-treatment particles in the large size range and the 20 μM dose resulted in approximately 47% of particles in the large size range. These treatment conditions also resulted in the largest increases of percentages between pre- and post-treatment. A 35% and 34% increase for the 50 μM and 100 μM doses was observed, respectively. At pH 7.5, only the 100 μM dose with high algae concentration resulted in a

post-treatment large particle percentage in a similar range to the low pH (48%). As seen in the figure, this represented a 31% increase in large particles.

Reduction in total particle counts and shifts in size distribution are mainly attributed to the expected presence of in-situ formed ferric hydroxide ($Fe(OH)_3$). The potential formation of insoluble $Fe(III)$ species through reduction of ferrate and their benefit to coagulation is further discussed in **Section 3.1.4**. Additionally, reduction in total particle counts and shifts in the size distribution could also be attributed to the release of extracellular organic matter (EOM) from algae cells in response to ferrate oxidation (Ma & Liu, 2002). As proposed by Ma and Liu, this EOM could behave like anionic and non-ionic polyelectrolytes that would work as a coagulant aid secreted to agglomerate inactivated algal cells (Ma & Liu, 2002).

It is important to note that some large particles were also observed floating on the water surface of post-treatment samples. These particles are believed to have been larger than the size ranges captured by the PC5000 counter and are not reflected in the figures included in this report.

3.1.2 UV$_{254}$ Absorbance

The average UV$_{254}$ absorbance was measured before and after oxidation with potassium ferrate. UV$_{254}$ absorbance for pre-treatment samples containing low algae particle counts typically ranged from 0.002 to 0.006 1/cm. The absorbance for pre-treatment samples containing high algae particle counts typically ranged from 0.004 to 0.017 1/cm. Average UV$_{254}$ absorbance results for pre- and post-treatment samples at pH 6.2 and a low or high algae concentration are presented in Figure 11 and Figure 12, respectively.
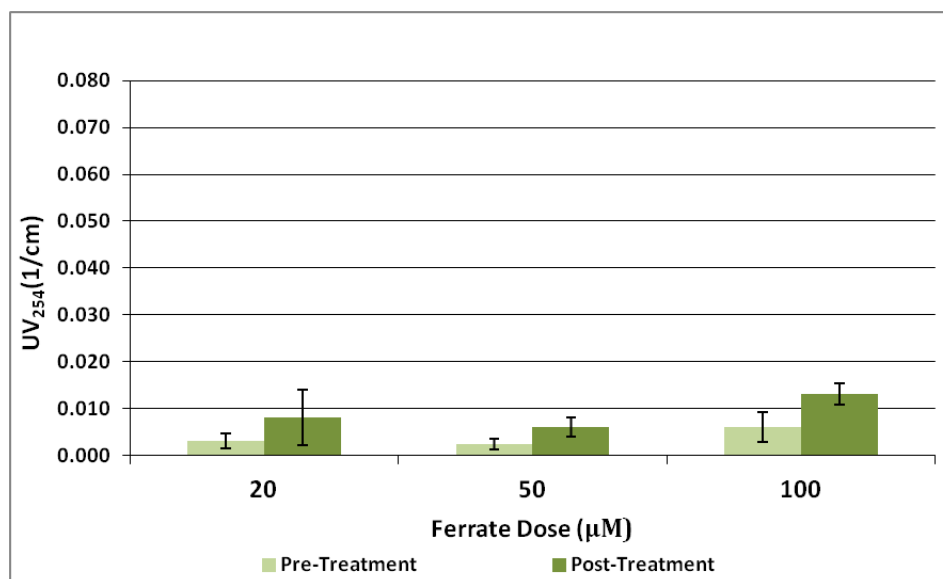
Figure 11: Average UV$_{254}$ Absorbance for Low Algae (pH 6.2)
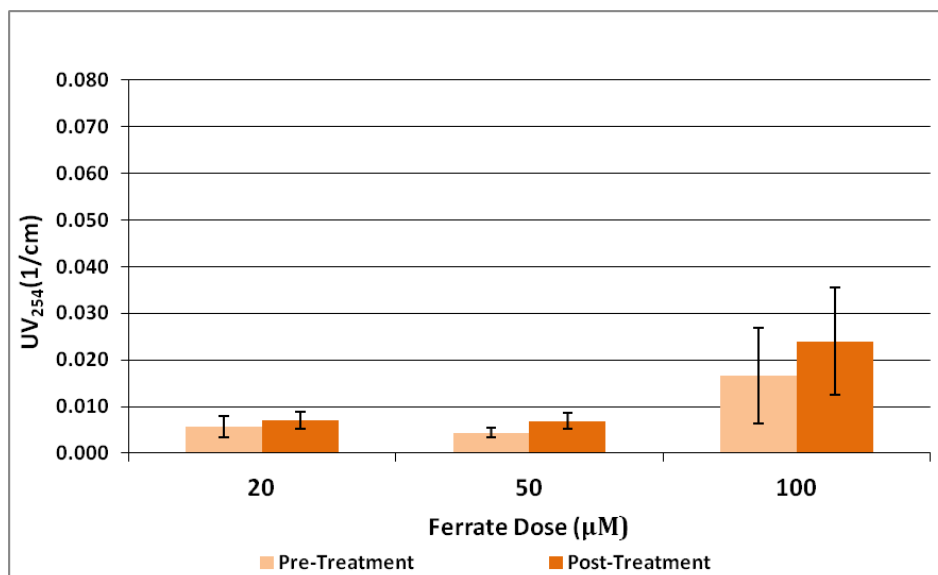
Figure 12: Average UV_{254} Absorbance for High Algae (pH 6.2)

An increase in UV_{254} was observed under all ferrate dosing conditions for both low algae and high algae waters at pH 6.2, as seen in the figures. As seen in Figure 11, the largest increase in absorbance for low algae was observed during the 100 μM dose (0.007 1/cm), which could indicate the occurrence of cell lysis and the release of chromophoric organic matter. As seen in Figure 12, the largest increase in absorbance for high algae was also observed during the 100 μM dose (0.007 1/cm).

Results for pre- and post-treatment samples at pH 7.5 and a low or high algae concentration are presented in Figure 13 and Figure 14, respectively.
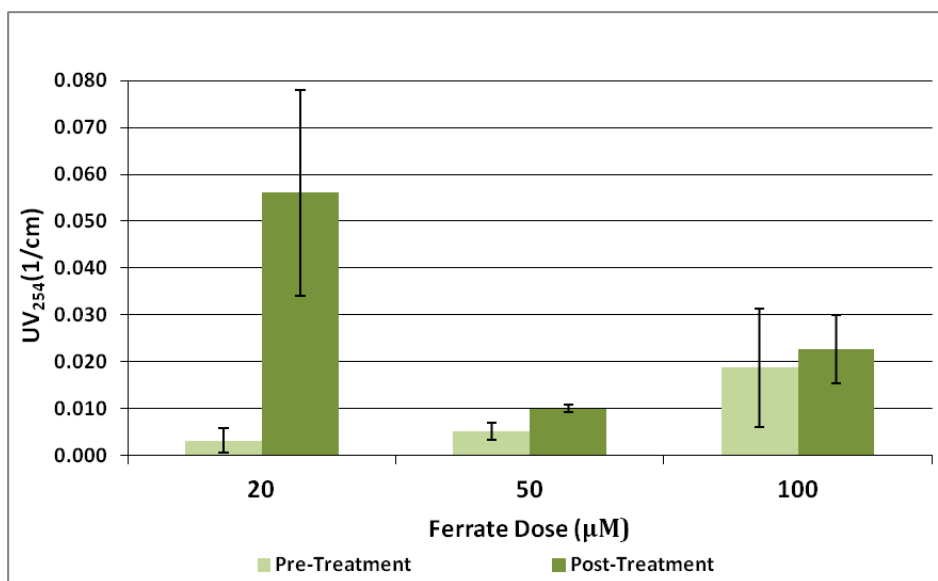
Figure 13: Average UV_{254} Absorbance for Low Algae (pH 7.5)
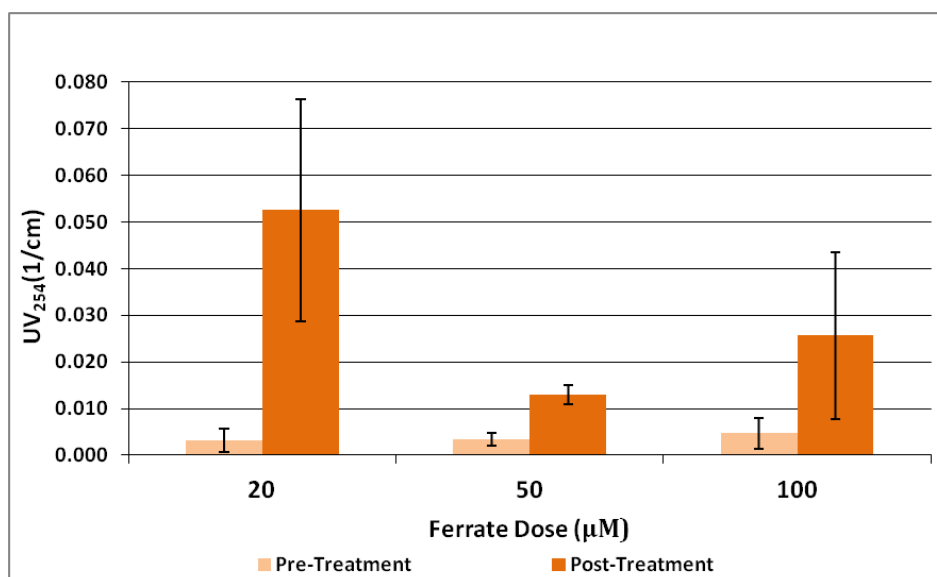
Figure 14: Average UV_{254} Absorbance for High Algae (pH 7.5)

An increase in UV_{254} absorbance was also observed under all ferrate dosing conditions for both low algae and high algae waters at pH 7.5, as seen in the figures. As seen in Figure 13, the largest increase in absorbance for low algae waters was observed during the 20 μM dose (0.053 1/cm), which could indicate the occurrence of cell lysis and the release of chromophoric organic matter. As seen in Figure 14, the largest increase in absorbance for high algae waters was also observed during the 20 μM dose (0.05 1/cm). As seen in both figures, a similar pre-treatment and post-treatment absorbance value was observed in samples for each dosing condition, regardless of algae concentration.

In prior studies by Ma & Liu (2002), an increase in UV_{254} absorbance after oxidation with Fe(VI) was also observed in waters containing the algae species *Scenedesmus* and *Chlorococoum*. It is proposed that an increase in UV absorbance could either indicate an increase in dissolved organic carbon (DOC) by the release of IOM or a structural change of existing EOM (Ma & Liu, 2002). A discussion on DOC is presented in **Section 3.1.3**.

3.1.3 Total Organic Carbon & Dissolved Organic Carbon

The total organic carbon (TOC) and dissolved organic carbon (DOC) were measured in pre-treatment and post-treatment samples. As expect, waters with a higher algae concentration had higher pre-treatment TOC concentrations. Pre-treatment TOC for water samples with 20,000 pc/mL algae concentration ranged from 0.026 to 0.215 mg/L. Pre-treatment TOC for water samples with 100,000 pc/mL algae concentration ranged from 0.363 to 0.654 mg/L.

Three scenarios were considered in the analysis of TOC and DOC results:

1. An increase in TOC with a corresponding increase in DOC in post treatment samples indicated the possible release of dissolved intracellular organic matter (IOM) without subsequent oxidation of IOM and existing extracellular organic matter (EOM) to non-dissolved organic compounds.
2. An increase in TOC with a corresponding decrease in DOC in post-treatment samples indicated the possible release of dissolved IOM with subsequent coagulation of IOM and existing EOM to particulate organic compounds.
3. A decrease in TOC with a corresponding decrease in DOC indicated the possible release of dissolved IOM with subsequent oxidation of IOM and EOM to CO_2 gas, which would be removed during sample sparging.

Table 2 presents the pre-treatment and post-treatment TOC and DOC concentrations for a pH of 6.2. In the table, an increase or decrease in TOC and/or DOC is represented by an upward or downward arrow, as appropriate. For a low algae concentration, the 20 μM Fe(VI) dose produced a decrease in TOC and a decrease in DOC (0.034 to 0.014 mg/L for TOC and 0.068 to 0.001 mg/L for DOC). As discussed above, this could indicate that dissolved organic matter was oxidized into CO_2 and removed from the sample during sparging. Due to the low Fe(VI) dose, it is likely that algal cells did not release IOM, but rather existing dissolved EOM was oxidized to CO_2. The 50 μM dose produced an increase in both TOC and DOC (0.026 to 0.179 mg/L for TOC and 0.047 to 0.076 mg/L for DOC). This indicates that algae cells released dissolved IOM; however, significant subsequent oxidation of released IOM and/or existing EOM did not occur. Finally, the 100 μM Fe(VI) dose produced an increase in TOC and a decrease in DOC (0.036 to 0.172 mg/L for TOC and 0.101 to 0.085 mg/L for DOC). As previously discussed, this could indicate that algae cells released dissolved IOM, which was subsequently coagulated with existing EOM into particulate organic compounds.

For a high algae concentration, both the 20 μM and 100 μM Fe(VI) doses produced an increase in TOC and a decrease in DOC (0.500 to 0.587 mg/L for TOC and 0.172 to 0.156 mg/L for DOC (20 μM), 0.405 to 0.766 mg/L for TOC and 0.213 to 0.144 mg/L for DOC (100 μM)). This indicates that algae cells released dissolved IOM, which was subsequently coagulated with existing EOM into particulate organic compounds. The 50 μM Fe(VI) dose produced an increase in both TOC and DOC (0.654 to 0.813 mg/L for TOC and 0.171 to 0.265 mg/L for DOC), indicating a release of dissolved IOM without subsequent coagulation of this organic matter to particulate organic compounds or oxidized to CO_2.

Table 2: TOC and DOC Concentration (pH 6.2)

| Algae | Fe(VI) | Pre-Treatment | | Post-Treatment | | ΔTOC | ΔDOC |
		Avg TOC (mg/L)	Avg DOC (mg/L)	Avg TOC (mg/L)	Avg DOC (mg/L)		
Low	20	0.034	0.068	0.014	0.001	↓	↓
Low	50	0.026	0.047	0.179	0.076	↑	↑
Low	100	0.036	0.101	0.172	0.085	↑	↓
High	20	0.500	0.172	0.587	0.156	↑	↓
High	50	0.654	0.171	0.813	0.265	↑	↑
High	100	0.405	0.213	0.766	0.144	↑	↓

Similarly, Table 3 presents the pre-treatment and post-treatment TOC and DOC concentrations for pH 7.5. In the table, an increase or decrease in TOC and/or DOC is represented by an upward or downward arrow, as appropriate. For a low algae concentration, the 20 μM Fe(VI) dose produced a decrease in both TOC and DOC (0.215 to 0.198 mg/L for TOC and 0.242 to 0.179 mg/L for DOC). As discussed above, this could indicate that dissolved organic matter was oxidized into CO_2 and removed from the sample during sparging. Due to the low Fe(VI) dose, it is likely that algal cells did not release IOM, but rather existing dissolved EOM was oxidized to CO_2. Both the 50 μM and 100 μM Fe(VI) doses produced an increase in TOC and a decrease in DOC (0.214 to 0.261 mg/L for TOC and 0.213 to 0.178 mg/L for DOC (50 μM), 0.032 to 0.0756 mg/L for TOC and 0.053 to 0.017 mg/L for DOC (100 μM)). This indicates that dissolved IOM was released by algae cells and was subsequently coagulated into particulate organic compounds.

For a high algae concentration, both the 20 μM and 50 μM Fe(VI) doses produced an increase in both TOC and DOC (0.406 to 0.613 mg/L for TOC and 0.009 to 0.092 mg/L for DOC (20 μM), 0.542 to 0.646 mg/L for TOC and 0.192 to 0.340 mg/L for DOC (50 μM)). This indicates that algae cells released dissolved IOM; however, significant subsequent coagulation or oxidation of released IOM and/or existing EOM did not occur. Finally, the 100 uM Fe(VI) dose produced an increase in TOC and a decrease in DOC (0.363 to 0.596 mg/L for TOC and 0.071 to 0.001 mg/L for DOC), indicating that dissolved IOM was released by algae cells and was subsequently coagulated into particulate organic compounds.

Table 3: TOC and DOC Concentration (pH 7.5)

Algae	Fe(VI)	Pre-Treatment		Post-Treatment		ΔTOC	ΔDOC
		Avg TOC (mg/L)	Avg DOC (mg/L)	Avg TOC (mg/L)	Avg DOC (mg/L)		
Low	20	0.215	0.242	0.198	0.179	↓	↓
	50	0.214	0.213	0.261	0.178	↑	↓
	100	0.032	0.053	0.075	0.017	↑	↓
High	20	0.406	0.009	0.613	0.092	↑	↑
	50	0.542	0.192	0.646	0.340	↑	↑
	100	0.363	0.071	0.596	0.001	↑	↓

Under all conditions the 100 μM Fe(VI) dose produced an increase in TOC and a decrease in DOC. This indicates that this dose is capable of causing cell lysis; however, it can provide subsequent coagulation of released matter into particulate organic compounds. At both pH conditions and low algae, the 20 μM Fe(VI) dose produced a reduction of both TOC and DOC. This indicates that algae cells were likely not releasing IOM and only the existing EOM was being oxidized to CO_2 and was sparged from the sample. The 50 μM Fe(VI) dose most frequently resulted in the release of dissolved organic matter into the water without subsequently oxidizing it to CO_2 or other non-dissolved organic compounds. This correlates to findings by the University of Rhode Island (URI), where IOM release was also observed under both pH conditions. However, URI concluded that further oxidation occurs more frequently at pH 6.2, where it appears equally as frequently in these results. Previous studies observed up to a 67% reduction in DOC through subsequent oxidation in algae containing waters (Liu et al., 2017).

It is important to note that due to mechanical difficulties with the Shimadzu TOC-5000A Analyzer, duplicate tests were not performed for TOC and DOC experiments. Values presented in this section are based on a single set of experiments. Further TOC and DOC testing should be performed to provide replicates for this data.

3.1.4 Total Iron and Post-Oxidation Iron Fractionation

The total iron concentration was determined for pre and post-treatment samples. The total iron for pre-treatment samples prior to ferrate dosing ranged from 0.01 mg/L-Fe to 0.07 mg/L-Fe. This was used as the baseline iron present in post-treatment samples. The total iron of post-treatment samples was used to calculate the actual dose as ferrate applied to samples during oxidation and whether or not the actual ferrate dose was within 25% of the intended ferrate dose. Tests that resulted in an actual ferrate dose that differed from the intended dose by 25% or more were discarded and repeated. The total iron concentrations

in post-treatment samples that were expected for each ferrate dose are provided in Table 4, below.

Table 4: Expected Total Iron Concentrations by Ferrate Dose

Dose (µM Fe(VI))	Total Iron (mg/L-Fe)
20	1.12
50	2.79
100	5.59

Iron fractionation was determined by a series of filtering and classifying iron species as large particulate, small particulate, colloidal, and dissolved. Large particulate iron was classified as not passing through a 0.7 µm filter and small particulate iron was classified as not passing through a 0.22 µm filter. Colloidal iron was classified as not passing through a 30 kDa ultrafilter. Dissolved iron was classified as the remaining iron after filtration through the 30 kDa ultrafilter.

As seen in Figure 15, below, the majority of iron particles did not pass through the 0.7 µm filter (90.9 to 99.3% of iron), indicating that mostly large particulate iron species were present in post-treatment samples at pH 6.2, regardless of ferrate dose or algae concentration. Over 90% of iron species were found to be in the large particulate state in every condition. The 20 µM ferrate dose resulted in the highest number of small iron particles, for both algae concentrations, at 9.1% for the low algae concentration and 2.4% for the high algae concentration. Insignificant concentrations of colloidal particulate iron (less than 0.8%) were observed in samples with both low and high algae. No dissolved iron was present for any dosing conditions at pH 6.2.
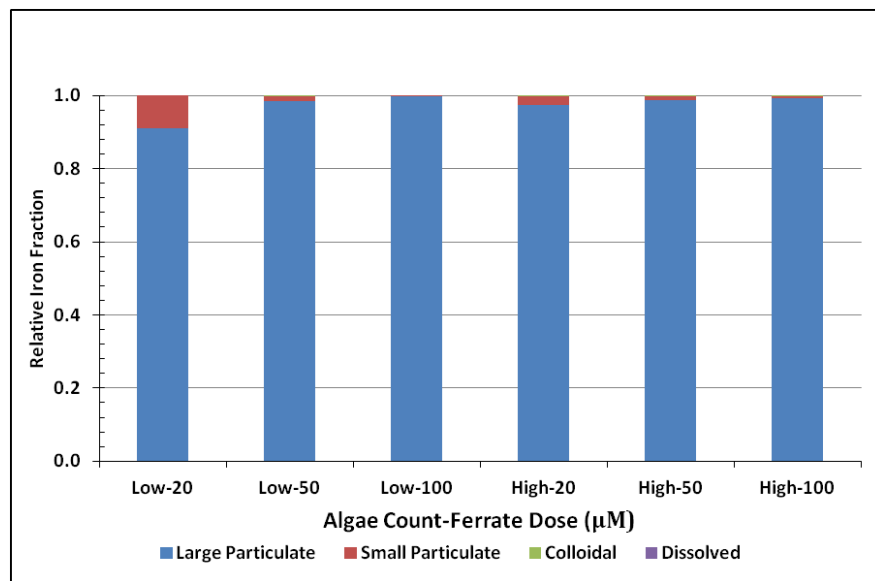
Figure 15: Relative Average Iron Fractionation (pH 6.2)

As seen in Figure 16, the distribution of iron species present in post-treatment samples at pH 7.5 was greater than at pH 6.2. For low algae samples, small particulate iron and colloidal iron species were observed, in addition to large particulate iron, at all ferrate doses. Dissolved iron was observed after treatment with the 20 μM dose with a low algae concentration. The 20 μM dose also resulted in the highest percent of small iron particles in low algae samples (average of 22%). Samples with low algae and a 100 μM dose had the highest percent of large particles (average of 99%) and very small percents of small, colloidal, and dissolved iron. For samples with high algae, the majority of iron particles did not pass through the 0.7 μm filter (75-100% of iron), indicating that iron particles were large after treatment. However, small and colloidal iron species were present after treatment with the 20 and 50 μM doses.
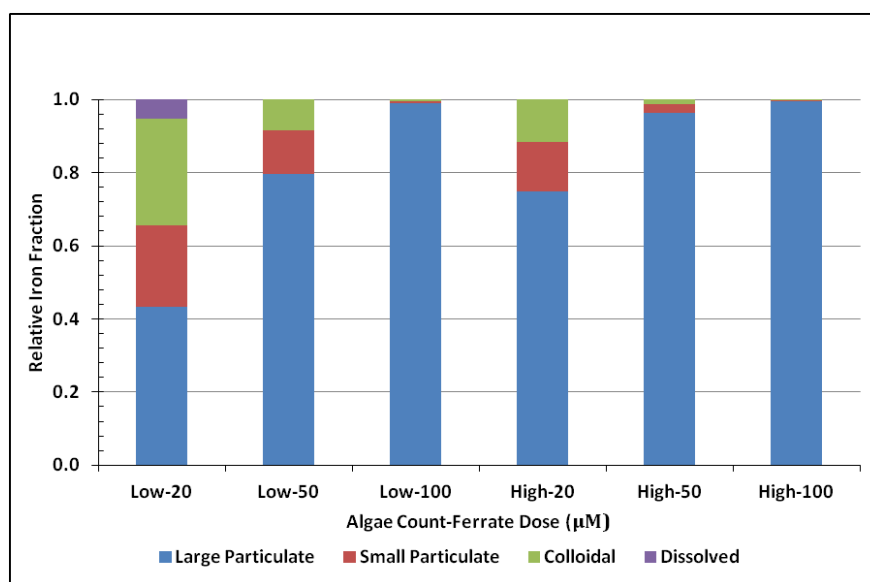
Figure 16: Relative Average Iron Fractionation (pH 7.5)

The presence of large particulate iron could indicate the formation of insoluble Fe(III) and Fe(II) compounds after the reduction of Fe(VI) during the oxidation process. The formation of iron (III) hydroxide flocs is commonly relied on during waste water and drinking water treatment processes to remove suspended materials. If Fe(III) is present, the formation of insoluble iron (III) hydroxide is possible, especially at neutral to acidic water conditions. This is evidenced in the high percentage (greater than 90%) of large iron particles at pH 6.2. Additionally, as shown in both figures, the percent of large particulate iron increased with increasing Fe(VI) dose, regardless of pH and algae concentration.

This could also partially explain the reduction in total particle counts and shift in particle size distribution discussed in **Section 3.1.1**. The expectation for the formation of ferric hydroxide colloids during oxidation is supported through findings by Zhou et al. (2016),

33

who used scanning electron microscopy (SEM) to image post ferrate treatment particles at pH 6.

Samples that had high dissolved iron species left over in solution generally continued to have a purple hue throughout reaction. This indicates the presence of unreacted K_2FeO_4 and the presence of Fe(VI) ions, which are more stable at higher pH values. Fe(VI) decay is discussed in further detail in **Section 3.1.6**. Samples that contained a high concentration of large particulate iron generally had an orange hue after reaction.

3.1.5 Total Nitrogen

The total nitrogen (TN) concentration was analyzed in pre- and post-treatment samples. The comparison of pre-treatment to post-treatment TN results can indicate different outcomes of treatment and the presence of nitrogen rich intracellular organic matter (IOM). An increase in TN concentration after Fe(VI) treatment can indicate cell lysis and the release of nitrogen rich IOM into the water. A constant TN concentration could indicate successful treatment of algae without the occurrence of cell lysis and release of IOM. Alternatively, no change in TN concentration could indicate cell lysis with the transformation of IOM to other forms of nitrogen, including ammonia and nitrogen gas. However, ammonia concentration was found to be negligible in these experiments. A reduction in TN concentration is significant, as it could mean a reduced probability for the formation of nitrogenous disinfection by-products (N-DBPs). As previously discussed, N-DBPs can be two to three orders of magnitude more toxic than halogenated DBPs.

Figure 17 presents the pre- and post-treatment TN concentrations at a pH of 6.2. As seen in the figure, TN concentrations were reduced after Fe(VI) oxidation under all dosing conditions. As expected, waters with higher starting concentrations of algae contained higher pre-treatment TN concentrations than those with lower algae concentrations. The pre-treatment TN concentration ranged from 0.024 to 0.067 mg-N/L for low algae waters and from 0.13 to 0.17 mg-N/L for high algae waters. The 20 and 50 µM Fe(VI) doses were capable of oxidizing TN concentrations to non-detectable levels, while the 100 µM Fe(VI) dose reduced TN to approximately 0.014 mg-N/L for low algae waters. At the high algae concentration, the 20 µM Fe(VI) dose reduced TN to 0.086 mg-N/L, the 50 µM Fe(VI) dose reduced TN to 0.097 mg-N/L, and the 100 µM Fe(VI) dose reduced TN to 0.067 mg-N/L.
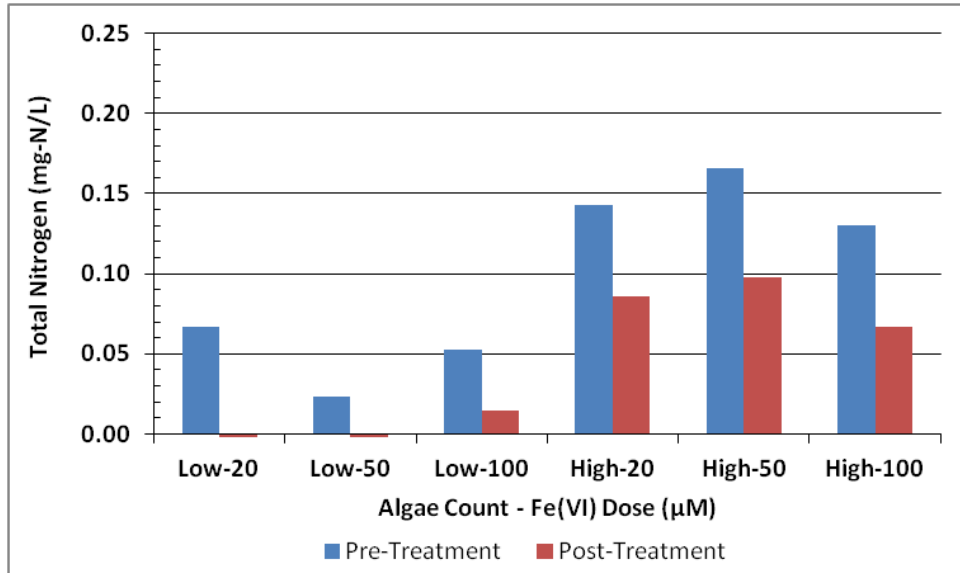
Figure 17: Total Nitrogen (pH 6.2)

Figure 18 shows the pre- and post-treatment TN concentrations at a pH of 7.5. As seen in the figure, TN was reduced under both algae conditions and all Fe(VI) doses. For the low algae concentration, the 20 μM Fe(VI) dose reduced TN to approximately 0.046 mg-N/L, the 50 μM Fe(VI) dose reduced TN to 0.056 mg-N/L, and the 100 μM Fe(VI) dose reduced TN to non-detectable levels. At the high algae concentration, the 20 μM Fe(VI) dose reduced TN to approximately 0.156 mg-N/L, the 50 μM Fe(VI) dose reduced TN to 0.075 mg-N/L, and the 100 μM Fe(VI) dose reduced TN to non-detectable levels. The TN for the 20 μM Fe(VI) dose was the highest concentration observed under any testing conditions.
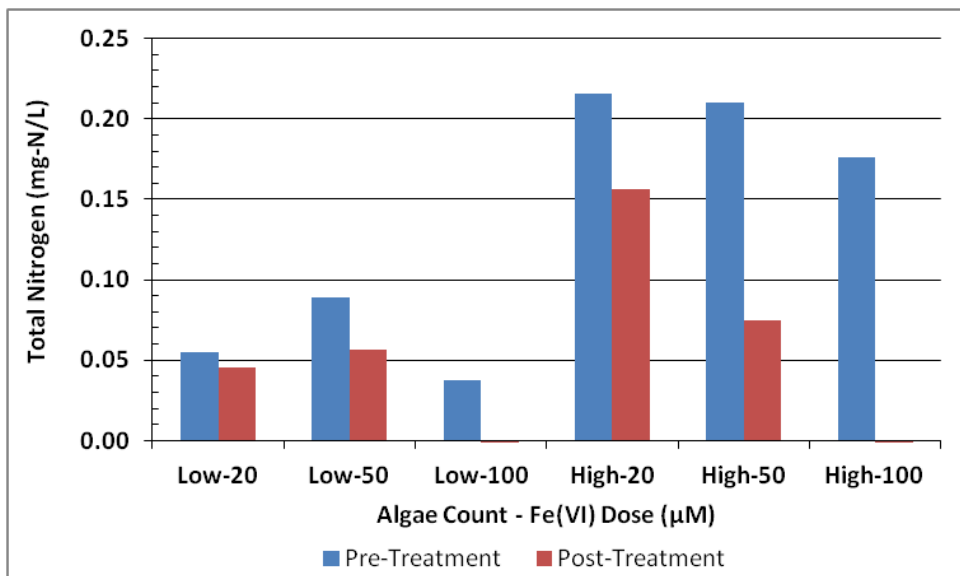
Figure 18: Total Nitrogen (pH 7.5)

It is important to note that due to nitrogen contamination of the test reagents, duplicate tests were not performed for TN experiments. Values presented in this section are based on a single set of experiments. Further TN testing should be performed to provide replicates for this data.

3.1.6 Ferrate Decay

3.1.6.1 Performed with 1mM Bicarbonate Buffer
Post-treatment samples were taken at set time intervals after dosing 1 mM buffered raw water with potassium ferrate and tested for ferrate concentration via the ABTS test method. 1 mM bicarbonate buffer concentration was the standard for all experiments performed. Absorbance data from the ABTS test was converted to concentration of Fe(VI) (μM) as discussed in **Section 2.3.6**.

Figure 19 shows the Fe(VI) decay curves for a 20, 50, and 100 μM Fe(VI) dose in waters with low algae and pH 6.2 (Experiment 1E, 2C, and 3B, respectively). As seen in the figure, Fe(VI) decays rapidly in waters with a pH 6.2, regardless of dose, and typically reached completion at 10 minutes. The residual Fe(VI) concentration remaining in the post-treatment samples increased with increasing initial dose and ranged from 3.9 to 13.0 μM. Similar Fe(VI) decay results were also observed for each dose in waters with a high algae concentration at pH 6.2. The residual Fe(VI) concentration remaining in post-treatment samples at the high algae concentration also increased with increasing initial dose and ranged from 3.1 to 16.2 μM.
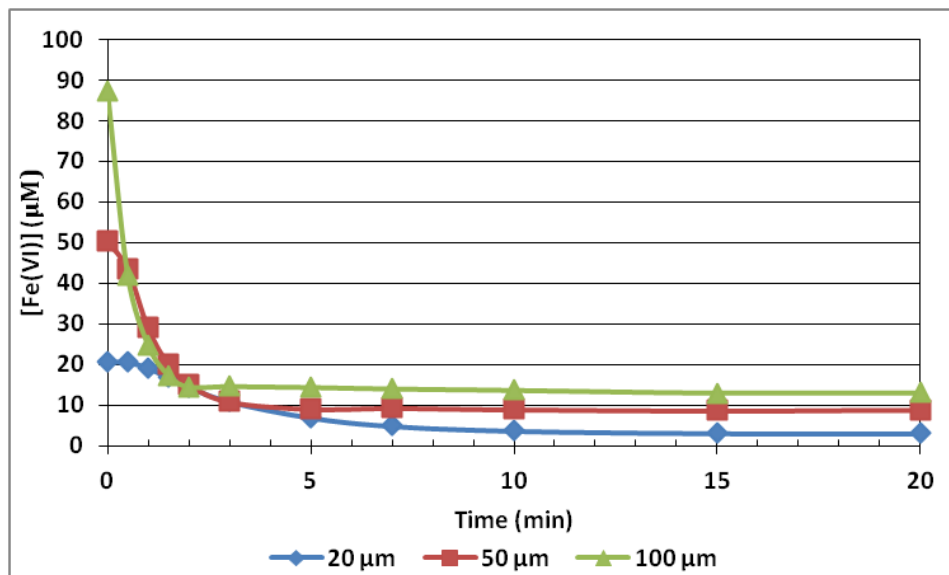
Figure 19: Fe(VI) Decay Curves with Low Algae Concentration (pH 6.2)

Figure 20 shows the Fe(VI) decay curves for a 20, 50, and 100 μM Fe(VI) dose in waters with low algae and pH 7.5 (Experiment 7B, 8B, and 9B, respectively). As seen in the figure, the Fe(VI) decay rate was slower than in waters with a pH 6.2. Although the decay rate increased with increasing initial dose, the decay rate of the 100 μM dose was still slower than any of the rates observed at pH 6.2. This was in agreement with other studies (Jiang et al., 2015). This lag in Fe(VI) decay was expected since Fe(VI) ions are more stable at higher pH values, as discussed in **Section 3.1.4**. At pH 7.5, appreciable Fe(VI) decay appeared to continue to approximately 25 minutes after dosing. The residual Fe(VI) concentration remaining in post-treatment samples for all doses was approximately 10 μM. Similar Fe(VI) decay results were also observed for each dose in waters with a high algae concentration at pH 7.5. The residual Fe(VI) concentration remaining in post-treatment samples at the high algae concentration was also approximately 10 μM for all doses.
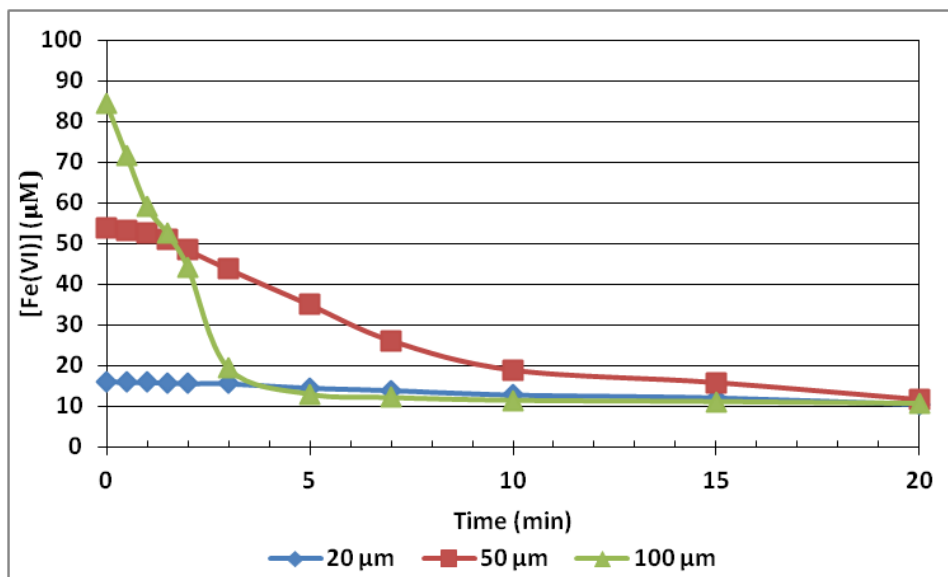
Figure 20: Fe(VI) Decay Curves with Low Algae Concentration (pH 7.5)

Concentration data for the experiments depicted in Figure 19 and Figure 20 was linearized and graphed with the equations in Table 5. A line of best fit was produced for each linearized graph and the coefficient of determination (R^2) values were compared to determine which order of reaction ferrate decay follows.

Table 5: Linearized Equations to Determine Reaction Order Graphically

Reaction Order	Linearized Equation	Plot X-axis	Plot Y-axis
Zero	$C=C_0-kt$	Time (t)	C
First	$\ln(C)=\ln(C_0)-kt$	Time (t)	$\ln(C)$
Second	$1/C=1/C_0 +kt$	Time (t)	1/C

For pH 6.2, linearized data for all doses and algae conditions did not fit any of the reaction order models. For pH 7.5, linearized data for the 100 μM dose for both low and high algae waters also did not fit any of the reaction order models. The 20 and 50 μM doses with low and high algae at pH 7.5 distinctly fit either a first-order model or a second-order model, or fit both essentially equally. Table 6 presents the R^2 values for the linearized data of tests performed with low and high algae and doses of 20 and 50 μM Fe(VI) at pH 7.5. As seen in the table, the 20 μM dose with low algae fit both a first- and second-order model; the 50 μM dose with low algae fit a second-order model, the 20 μM dose with high algae fit a first-order model, and the 50 μM dose fit both a first- and second-order model. There is disagreement among the literature over the correct reaction order for Fe(VI) decomposition, with some observing that Fe(VI) follows a mixed first- and second-order model while other have reported only a second-order decomposition rate (Jiang et al., 2015). This may explain the inconsistency observed between reaction orders in these experiments.

Table 6: Coefficients of Determination (R^2) for Selected Rate Data

Test	Coefficient of Determination (R^2)		
	Zzero Order	1St Order	2nd Order
Low – 20 (7B)	0.9863	0.9932	0.9925
Low – 50 (8B)	0.8850	0.9612	0.9921
High – 20 (10A)	0.9786	0.9930	0.9487
High – 50 (11B)	0.8974	0.9748	0.9728

Reaction rate and reaction completion time are important for treatment plant operators during the application of ferrate for pre-oxidation. Raw water pH conditions and pH requirements for downstream treatment methods may dictate at what pH value pre-oxidation with ferrate would occur and could impact the rate of reaction.

3.1.6.2 Performed with 2 mM Bicarbonate Buffer and 50 μM Ferrate Dose

The second set of Fe(VI) decay tests were conducted at a bicarbonate buffer concentration of 2 mM, pH of 7.5, and Fe(VI) dose of 50 μM to specifically compare with tests performed by Jiang et al. (2015), who studied the effects of natural organic matter (NOM) on Fe(VI) decomposition. The Fe(VI) tests were performed on raw water with a 0, 20,000, or 100,000 pc/mL algae concentration to specifically see if the presence of algae changed the rate of decomposition of Fe(VI). Experiments were not performed under these conditions at a pH of 6.2, due to the very rapid rate of decomposition witnessed in tests performed with a 1 mM bicarbonate buffer concentration. As seen in the Fe(VI) decay curves depicted in Figure 21, an algae concentration of 100,000 pc/mL slightly decreased the rate of Fe(VI) decay. These results correlate with the findings of Jiang et al. (2015), where the presence of NOM acted as a stabilizer to Fe(VI) decomposition. A decrease in decay rate could be attributed to intracellular and extracellular organic matter coating the surface of ferrate particles or

by it altering the surface area available for decomposition as witness with natural organic matter in the Jiang et al. (2015) experiments.
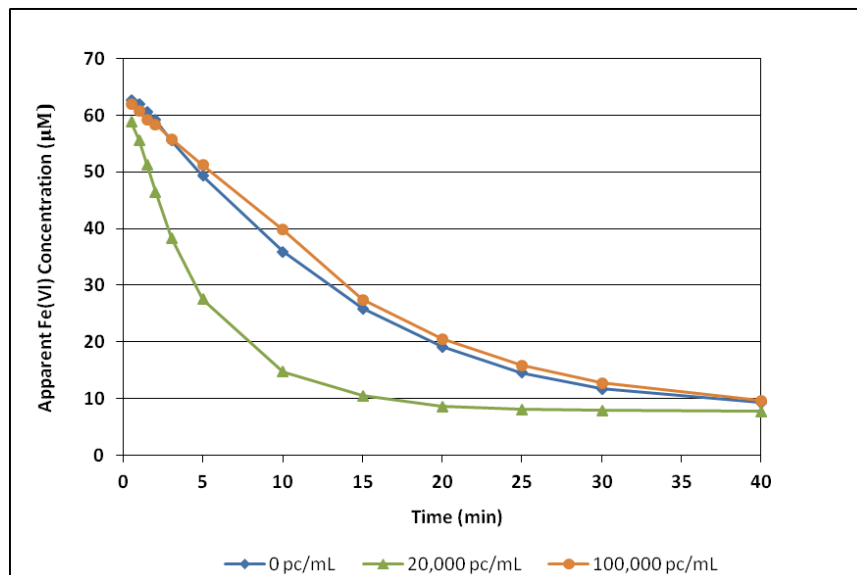
Figure 21: Fe(VI) Decay Curves with 2 mM Bicarbonate Buffer (pH 7.5)

As seen in the figure, an increased Fe(VI) decay rate was observed with an algae concentration of 20,000 pc/mL. As discussed by Jiang et al. (2015), the presence of NOM was expected to increase the rate of Fe(VI) decomposition through redox reactions; however, it actually acted as a stabilizer. It is possible that an algae concentration of 20,000 pc/mL provided enough organic matter for redox reactions to increase the Fe(VI) decay rate but not so much that it coated the surface of ferrate particles or altered the surface area available for Fe(VI) decomposition. It is expected that increasing algae concentration in increments up to 100,000 pc/mL would result in decay rates approaching the natural decomposition rate of Fe(VI).

The concentration data for the no-algae condition shown in Figure 21 was linearized and fit to reaction rate models with the method described in **Section 3.1.6.1**. The concentration data fit the first-order reaction model with an R^2 value of 0.9816 and the second-order model with an R^2 value of 0.9826. The similarity between the fits to both a first- and second-order rate model agrees with Jiang et al. (2015). The rate data for Fe(VI) decay in the presence of 20,000 pc/mL algae could not be represented by any of the rate models. Finally, the rate data for Fe(VI) decay in the presence of 100,000 pc/mL was most accurately represented by a first order model with an R^2 value of 0.9879 but also had an R^2 value of 0.9758 for the second order model. These results agree with the proposition that Fe(VI) decomposition can be described as a mixed first- and second-order reaction, as discussed previously.

3.2 Impact of pH on Results

The post-treatment conditions for total particle counts, particle size, iron fractionation, and UV_{254} absorbance were generally more favorable in waters at pH 6.2. More favorable post-treatment conditions were considered to be those that provided algae removal without production of organic material that could potentially adversely impact downstream treatment processes. As previously discussed, the highest percent of total particle count reduction and the greatest shifts in percentage of large particles occurred at this pH. For treatment plant operations, the presence of larger particles would be more favorable in the downstream treatment processes of coagulation, flocculation, and sedimentation. The presence of mostly particulate iron under all dosing conditions at this pH indicates the formation of iron (III) species and the potential aid in downstream coagulation. Additionally, post-treatment UV_{254} absorbance was lower in samples at this pH, signifying less cell lysis occurring than at pH 7.5 and less organic material release into the water. This is important for downstream disinfection, especially with chlorine, as it indicates a reduced presence of disinfection byproduct precursors. Finally, the required treatment time for the oxidation reaction to reach completion was up to 20 minutes faster at pH 6.2 than at pH 7.5. This would allow more flexibility in treatment plant operation.

3.3 Impact of Raw Water Algae Concentration on Results

The concentration of algae in pre-treatment samples generally impacted reduction of particle counts, significance of particle size shifts, UV_{254} absorbance, TOC and DOC concentrations, and Fe(VI) decay. Greater shifts in particle size distribution to larger particles were observed at the higher algae concentration. Additionally, the high algae concentration resulted in higher percent removal of total particle counts. The higher algae concentration resulted in higher pre-treatment UV_{254} absorbance and generally higher post-treatment UV_{254} absorbance. As expected, the higher algae concentration provided higher pre-treatment TOC and DOC concentrations; however, Fe(VI) dose appeared to have a greater impact on the post-treatment TOC and DOC. Finally, the higher algae concentration was observed to have a stabilizing effect on Fe(VI) decay, similar to that of previous research performed with natural organic matter. This is attributed to coating of Fe(VI) particles which limits the surface area able to oxidize material. The lower algae concentration was observed to have increased the rate of Fe(VI) decay, possibly by providing oxidation reactions without coating the particles and limiting exposed surface area available for oxidation reactions.

3.4 Impact of Ferrate Dose on Results

Trends for post-treatment parameters by Fe(VI) dose were not as clearly defined as pH and algae concentration. Results for reduction in total particle counts, shifts in particle size distribution, and reduction in UV_{254} appeared to be more dependent on pH and algae concentration.

Chapter 4: Conclusions

4.1 Conclusions from Bench-Scale Testing

Results of this Fe(VI) oxidation study indicated that oxidation with ferrate does cause algal cell lysis and the release of IOM. It is predicted that some of this material can be further oxidized, depending on the Fe(VI) dose. Pre-oxidation with Fe(VI) also demonstrated marginal coagulation benefits by shifting particle sizes and possibly producing precipitated iron(III) species. Preliminary results also showed that Fe(VI) oxidation may reduce total nitrogen concentrations, which could reduce the potential for the formation of nitrogenous disinfection byproducts.

Fe(VI) oxidation performed at pH 6.2 generally provided more favorable post-treatment conditions. This means that algae removal was accomplished without high production of organic material that could potentially adversely impact downstream treatment processes. Fe(VI) oxidation at pH 6.2 provided the highest reduction in particle counts as well as the greatest shift in particle sizes. Additionally, Fe(VI) oxidation at pH 6.2 provided the large particulate iron species in post-treatment water. This could benefit treatment plant operations by enhancing coagulation, flocculation, and sedimentation processes downstream. Finally, the reaction rate for Fe(VI) oxidation occurred rapidly at pH 6.2.

4.2 Recommendations for Further Study

It is recommended that additional experimentation be completed for total organic carbon (TOC), dissolved organic carbon (DOC), and total nitrogen (TN) to provide replicates of data. As Fe(VI) oxidation was performed on a laboratory prepared water sample, it is recommended that further experimentation be performed with natural water samples. This will determine the impacts that other constituents like natural organic matter, alkalinity, and turbidity have on Fe(VI) oxidation.

Reference List

Anderson, D. M., Glibert, P. M., & Burkholder, J. M. (2002). Harmful algal blooms and eutrophication: Nutrient sources, composition, and consequences. *Estuaries*, *25*(4), 704–726. doi: 10.1007/bf02804901

Bare, WFR., Jones, N. B., & Middlebrooks, E. J. (1975). Algae Removal Using Dissolved Air Flotation. *Journal – Water Pollution Control Federation, 47(1),* 153-169.

Borchardt, J. A., & Omelia, C. R. (1961). Sand Filtration of Algal Suspensions. *Journal - American Water Works Association*, *53*(12), 1493–1502. doi: 10.1002/j.1551-8833.1961.tb00802.x

Campos, A., & Vasconcelos, V. (2010). Molecular Mechanisms of Microcystin Toxicity in Animal Cells. *International Journal of Molecular Sciences*, *11*(1), 268–287. doi: 10.3390/ijms11010268

Daly, R. I., Ho, L., & Brookes, J. D. (2007). Effect of Chlorination onMicrocystis aeruginosaCell Integrity and Subsequent Microcystin Release and Degradation. *Environmental Science & Technology*, *41*(12), 4447–4453. doi: 10.1021/es070318s

Dybas, C. (2019). Lake Erie's toxic algae blooms: Why is the water turning green?. National Science Foundation. Retrieved November 25, 2019 from https://www.nsf.gov/discoveries/disc_summ.jsp?cntn_id=298181

Edzwald, J. K. (1993). Algae, Bubbles, Coagulants, and Dissolved Air Flotation. *Water Science and Technology*, *27*(10), 67–81. doi: 10.2166/wst.1993.0207

Fertilizer Limits Sought Near Lake Erie to Fight Spread of Algae. (2014). *Nature Environment and Pollution Technology*, *13*(1), 132.

Ghernaout, B., Ghernaout, D., & Saiba, A. (2010). Algae and cyanotoxins removal by coagulation/flocculation: A review. *Desalination and Water Treatment*, *20*(1-3), 133–143. doi: 10.5004/dwt.2010.1202

Goodwill, J. E., Jiang, Y., Reckhow, D. A., & Tobiason, J. E. (2016). Laboratory Assessment of Ferrate for Drinking Water Treatment. *Journal - American Water Works Association*, *108*. doi: 10.5942/jawwa.2016.108.0029

He, X. K., Liu, Y.-L. D., Conklin, A. J., Westrick, J. J., Weavers, L. W., Dionysiou, D., … Walker, H. (2016). Toxic cyanobacteria and drinking water: Impacts, detection, and treatment. *Harmful Algae*, *54*, 174–193. doi: 10.1016/j.hal.2016.01.001

Jiang, W., Chen, L., Batchu, S. R., Gardinali, P. R., Jasa, L., Marsalek, B., … Sharma, V. K. (2014). Oxidation of Microcystin-LR by Ferrate(VI): Kinetics, Degradation Pathways, and Toxicity Assessments. *Environmental Science & Technology*, *48*(20), 12164–12172. doi: 10.1021/es5030355

Jiang, Y., Goodwill, J. E., Tobiason, J. E., & Reckhow, D. A. (2015). Effect of Different Solutes, Natural Organic Matter, and Particulate Fe(III) on Ferrate(VI) Decomposition in Aqueous Solutions. *Environmental Science & Technology*, *49*(5), 2841–2848. doi: 10.1021/es505516w

Lee, Y., Cho, M., Kim, J., & Yoon, J. (2004). Chemistry of Ferrate (Fe(VI)) in Aqueous Solution and its Applications as a Green Chemical. *Journal of Industrial and Engineering Chemistry, 10*(1), 161-171.

Lee, Y., Yoon, J., & Gunten, U. V. (2005). Spectrophotometric determination of ferrate (Fe(VI)) in water by ABTS. *Water Research*, *39*(10), 1946–1953. doi: 10.1016/j.watres.2005.03.005

Liu, S.-Y., Xu, J., Chen, W.-L., David, B. E., Wu, M., & Ma, F. (2017). Impacts of potassium ferrate(VI) on the growth and organic matter accumulation, production, and structural changes in the cyanobacterium Microcystis aeruginosa. *Environmental Science and Pollution Research*, *24*(12), 11299–11308. doi: 10.1007/s11356-017-8757-3

Ma, J., & Liu, W. (2002). Effectiveness and mechanism of potassium ferrate(VI) preoxidation for algae removal by coagulation. *Water Research*, *36*(4), 871–878. doi: 10.1016/s0043-1354(01)00282-2

Pimentel, J. S. M., & Giani, A. (2014). Microcystin Production and Regulation under Nutrient Stress Conditions in Toxic Microcystis Strains. *Applied and Environmental Microbiology*, *80*(18), 5836–5843. doi: 10.1128/aem.01009-14

United States Department of Commerce & National Oceanic and Atmospheric Administration (NOAA). (2019). Lake Erie Harmful Algal Bloom. Retrieved November 25, 2019, from https://www.weather.gov/cle/LakeErieHAB.

United States Environmental Protection Agency (EPA). (2015). Drinking Water Health Advisory for the Cyanobacterial Microcystin Toxins. *EPA 820R15100*. Office of Water, Washington, DC.

United States Environmental Protection Agency (EPA). (1993). Method 353.2, Revision 2.0: Determination of Nitrate-Nitrite Nitrogen by Automated Colorimetry. Office of Research and Development, Cincinnati, OH.

Wert, E. C., Dong, M. M., & Rosario-Ortiz, F. L. (2013). Using digital flow cytometry to assess the degradation of three cyanobacteria species after oxidation processes. *Water Research*, *47*(11), 3752–3761. doi: 10.1016/j.watres.2013.04.038

World Health Organization (WHO). (1999). "Recreational Waters." Toxic Cyanobacteria in Water: A Guide to Their Public Health Consequences, Monitoring, and Management. New York, New York.

Xie, P., Ma, J., Fang, J., Guan, Y., Yue, S., Li, X., & Chen, L. (2013). Comparison of Permanganate Preoxidation and Preozonation on Algae Containing Water: Cell Integrity, Characteristics, and Chlorinated Disinfection Byproduct Formation. *Environmental Science & Technology*, *47*(24), 14051–14061. doi: 10.1021/es4027024

Zhou, S., Shao, Y., Gao, N., Zhu, S., Li, L., Deng, J., & Zhu, M. (2014). Removal of Microcystis aeruginosa by potassium ferrate (VI): Impacts on cells integrity, intracellular organic matter release and disinfection by-products formation. *Chemical Engineering Journal*, *251*, 304–309. doi: 10.1016/j.cej.2014.04.081

Appendix A: Experimental Testing Plan
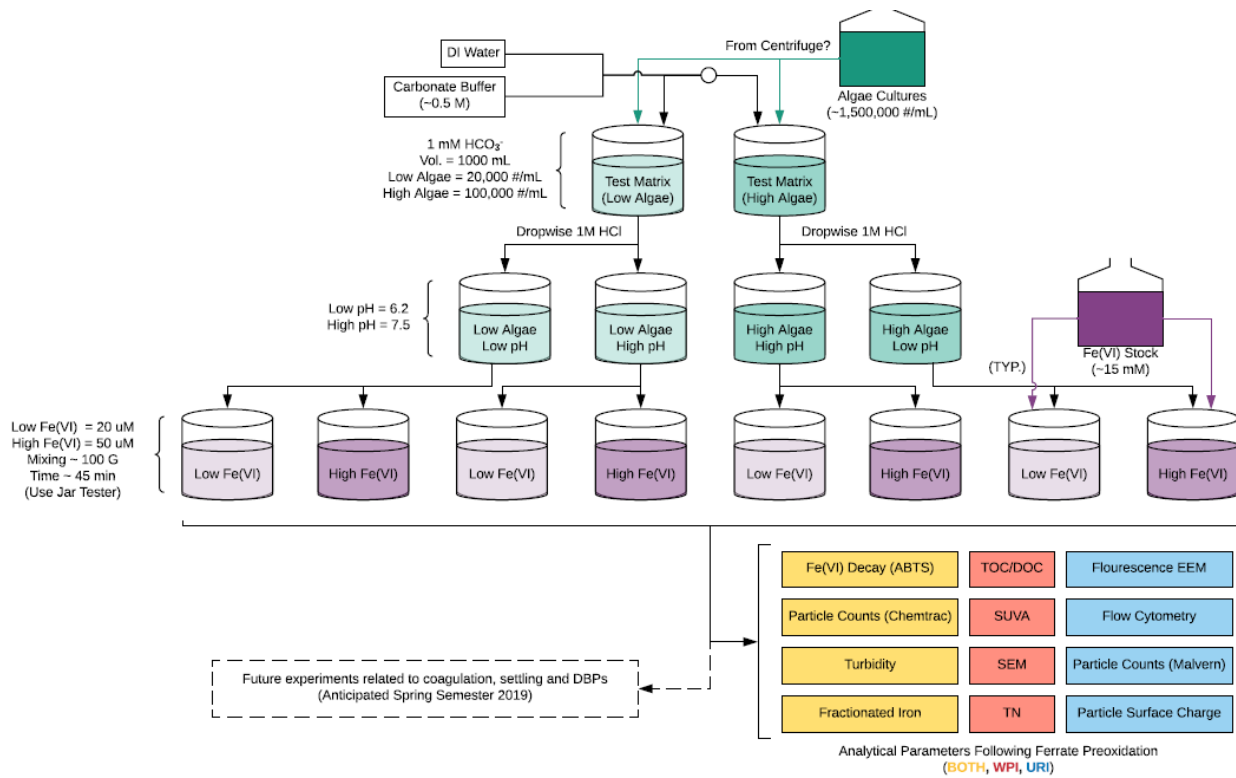
Note: Three ferrate doses were used during experimentation (not depicted in this figure) with doses of 20μM, 50μM, 100μM.

Appendix B: Analytical Results

B-1) Particle Count

Test	Pre 2um-3um	3um-6um	6um-9um	9um-16um	16um-27um	27um-44um	44um-75um	75um-125um	>125 um	TOTAL	Post 2um-3um	3um-6um	6um-9um	9um-16um	16um-27um	27um-44um	44um-75um	75um-125um	>125 um	TOTAL
1e	18,331	3,379	-99	100	0	0	0	0	0	21,711	6,108	2,629	101	100	50	0	0	0	0	8,988
1b	21,286	1,855	0	63	100	0	0	0	0	23,033	15,986	2,355	-71	13	0	0	0	0	0	18,283
1d	14,757	2,379	76	151	100	0	0	0	0	17,462	6,087	1,882	76	100	0	0	0	0	0	8,145
2a	25,931	953	88	150	50	0	0	0	0	27,171	10,131	7,903	1,838	600	0	0	0	0	0	20,471
2b	20,081	1,077	0	100	0	0	0	0	0	21,258	16,353	3,702	325	350	100	0	0	0	0	20,830
2c	20,107	1,079	-49	0	0	0	0	0	0	21,137	9,106	3,803	326	225	0	0	0	0	0	13,460
3a	24,575	1,492	0	0	0	0	0	0	0	25,696	2,182	829	51	0	0	0	0	0	0	3,062
3b	24,309	1,905	0	0	0	0	0	0	0	26,189	2,756	827	75	0	0	0	0	0	0	3,658
3d	17,935	2,106	-49	26	0	0	0	0	0	20,018	10,085	5,156	452	176	0	0	0	0	0	15,868
4a	70,182	41,304	301	0	0	0	0	0	0	111,763	5,857	5,578	425	100	0	0	0	0	0	11,960
4b	70,783	35,380	176	50	0	0	0	0	0	106,389	4,060	3,581	426	250	0	0	0	0	0	8,317
4d	89,134	12,156	-73	51	0	0	0	0	0	101,268	22,034	10,256	1,377	351	0	0	0	0	0	34,018
5e	82,239	19,557	26	26	0	0	0	0	0	101,847	14,389	11,907	2,026	676	50	0	0	0	0	29,047
5b	87,882	22,278	126	150	0	0	0	0	0	110,436	7,559	6,780	1,151	425	0	0	0	0	0	15,915
5d	80,484	18,130	76	150	50	0	0	0	0	98,890	5,558	5,680	1,951	1,100	50	0	0	0	0	14,338
6a	81,406	30,328	301	100	0	0	0	0	0	112,134	11,505	12,052	1,950	500	50	0	0	0	0	26,057
6b	81,313	13,028	26	50	0	0	0	0	0	94,417	16,658	9,703	1,300	400	100	0	0	0	0	28,160
6c	89,579	10,003	51	100	0	0	0	0	0	99,733	12,532	12,054	3,351	1,850	100	0	0	0	0	29,887
7a	18,329	4,052	200	300	150	0	0	0	0	23,030	20,082	5,403	451	300	100	0	0	0	0	26,335
7b	18,229	4,002	150	100	0	0	0	0	0	22,480	17,432	4,553	201	250	150	0	0	0	0	22,585
7d	14,710	4,683	-99	100	50	0	0	0	0	19,445	9,857	3,456	-49	100	0	0	0	0	0	13,365
8f	18,941	1,038	-97	301	200	0	0	0	0	20,383	5,588	1,809	102	26	0	0	0	0	0	7,525
8b	16,107	5,979	51	0	0	0	0	0	0	22,137	14,382	5,479	326	700	350	0	0	0	0	21,237
8e	17,210	2,130	51	150	50	0	0	0	0	19,591	9,406	4,454	526	1,100	650	0	0	0	0	16,135
9a	17,680	3,527	26	100	0	0	0	0	0	21,333	11,707	4,352	551	450	100	0	0	0	0	17,160
9b	22,082	3,255	51	0	0	0	0	0	0	25,387	9,056	6,228	1,426	850	100	0	0	0	0	17,659
9c	16,757	2,179	26	100	50	0	0	0	0	19,111	14,905	6,726	725	250	0	0	0	0	0	22,607
10a	80,255	18,703	101	125	50	0	0	0	0	99,233	64,482	13,778	226	200	100	0	0	0	0	78,786
10d	81,462	18,956	2	76	50	0	0	0	0	100,546	53,662	16,906	302	126	0	0	0	0	0	70,996
10c	86,985	14,207	-49	100	50	0	0	0	0	101,293	87,312	14,460	52	51	50	0	0	0	0	101,925
11d	84,134	18,803	26	150	0	0	0	0	0	103,113	16,934	11,553	1,976	650	150	0	0	0	0	31,263
11b	80,708	17,705	26	75	0	0	0	0	0	98,514	55,605	10,928	151	100	0	0	0	0	0	66,783
11c	83,715	16,736	-98	101	50	0	0	0	0	100,504	51,284	14,831	576	300	50	0	0	0	0	67,042
12a	83,631	13,604	26	25	0	0	0	0	0	97,286	9,956	9,278	2,626	1,350	50	0	0	0	0	23,260
12b	89,931	15,154	26	75	0	0	0	0	0	105,186	8,480	7,103	2,125	1,600	150	0	0	0	0	19,458
12c	81,537	23,082	-73	51	0	0	0	0	0	104,597	40,687	15,209	902	550	100	0	0	0	0	57,447

B-2) Total Organic Carbon & Dissolved Organic Carbon

pH	Algae	Fe(VI)	Test	Pre-Treatment Avg TOC (mg/L)	Pre-Treatment Avg DOC (mg/L)	Post-Treatment Avg TOC (mg/L)	Post-Treatment Avg DOC (mg/L)
6.2	Low	20	1	0.034	0.068	0.014	0.001
6.2	Low	50	2	0.026	0.047	0.179	0.076
6.2	Low	100	3	0.036	0.101	0.172	0.085
6.2	High	20	4	0.500	0.172	0.587	0.156
6.2	High	50	5	0.654	0.171	0.813	0.265
6.2	High	100	6	0.405	0.213	0.766	0.144
7.5	Low	20	7	0.215	0.242	0.198	0.179
7.5	Low	50	8	0.214	0.213	0.261	0.178
7.5	Low	100	9	0.032	0.053	0.075	0.017
7.5	High	20	10	0.406	0.009	0.613	0.092
7.5	High	50	11	0.542	0.192	0.646	0.340
7.5	High	100	12	0.363	0.071	0.596	0.001

B-3) Total Nitrogen

Test ID	TN Pre (mg-N/L)	TN Post (mg-N/L)
1	0.0673	-0.0028
2	0.0237	-0.1059
3	0.0528	0.0143
4	0.1425	0.0859
5	0.1660	0.0974
6	0.1300	0.0665
7	0.0551	0.0456
8	0.0886	0.0564
9b	0.0377	-0.1665
10a	0.2160	0.1560
11b	0.2100	0.0746
12b	0.1760	-0.0987

B-4) Iron Fractionation

pH	6.2																	
Algae Concentration (pc/mL)	20,000									100,000								
Fe(VI) Dose (µM)	20			50			100			20			50			100		
Test ID	1E	1b	1d	2a	2b	2c	3a	3b	3d	4a	4b	4d	5e	5b	5d	6a	6b	6c
Total Fe (mg/L -Fe)	1.39	1.04	1.29	2.92	2.63	2.82	6.14	4.88	6.2	1.33	1.15	1.33	3.18	2.98	3.18	6.72	5.36	6.12
Small Fe (Pass thru 0.7µm) (mg/L)	0.01	0.26	0.02	0.05	0.04	0.03	0.04	0	0.02	0.04	0.04	0.02	0.05	0.06	0.02	0.05	0.02	0.06
Colloidal Fe (Pass thru 0.22µm) (mg/L)	0	0	0	0		0.01	0	0	0.01	0	0	0.01	0.01	0	0.01	0.03	0	0.01
Dissolved (Pass thru UF) (mg/L)	0	0	0	0		0	0	0		0	0	0	0	0	0	0	0	0

pH	7.5																	
Algae Concentration (pc/mL)	20,000									100,000								
Fe(VI) Dose (µM)	20			50			100			20			50			100		
Test ID	7a	7b	7d	8f	8b	8e	9a	9b	9c	10a	10d	10c	11d	11b	11c	12a	12b	12c
Total Fe (mg/L -Fe)	1.03	0.9	1.15	2.94	3.26	3.14	5.24	6.72	6.44	1.19	1.33	1.26	2.88	2.92	3.14	6.02	6.24	6.2
Small Fe (Pass thru 0.7µm) (mg/L)	0.74	0.72	0.21	0.02	1.95	0.03	0.07	0.07	0.03	0.2	0.12	0.63	0.02	0.29	0.01	0.02	0.03	0.02
Colloidal Fe (Pass thru 0.22µm) (mg/L)	0.63	0.22	0.2	0.01	0.8	0.01	0.04	0.03	0.01	0.05	0.09	0.3	0	0.12	0	0.01	0.01	0.01
Dissolved (Pass thru UF) (mg/L)	0	0.09	0.07	0	0	0	0	0	0	0	0	0	0	0	0	0	0	0

B-5) UV$_{254}$ Absorbance

pH	Algae	Fe(VI)	Test	Pre-Treatment Absorbance				Group avg/ STDV	Post-Treatment Absorbance				Group avg/ STDV
				A	B	C	Avg		A	B	C	Avg	
pH 6.2	Low Algae	20	1e	0.003	0.003	0.002	0.003	0.003	0.013	0.005	0.005	0.0050	0.008
			1b	0.003	0.006	0.005	0.005	0.002	0.020	0.015	0.008	0.0143	0.006
			1d	0.003	0.009	0.001	0.002		0.005	0.004	0.005	0.0047	
		50	2a	0.003	0.002	0.001	0.002	0.002	0.01	0.003	0.005	0.0060	0.006
			2b	0.004	0.004	0.002	0.003	0.001	0.008	0.005	0.007	0.0067	0.002
			2c	0.002	0.003	0.001	0.002		0.005	0.005	0.006	0.0053	
		100	3a	0.004	0.008	0.004	0.005	0.006	0.017	0.012	0.01	0.0130	0.013
			3b	0.012	0.008	0.008	0.009	0.003	0.014	0.014	0.016	0.0147	0.002
			3d	0.003	0.004	0.003	0.003		0.013	0.011	0.011	0.0117	
	High Algae	20	4a	0.004	0.006	0.004	0.005	0.006	0.01	0.004	0.005	0.0063	0.007
			4b	0.006	0.003	0.004	0.004	0.002	0.006	0.007	0.007	0.0067	0.002
			4d	0.007	0.008	0.010	0.008		0.009	0.007	0.008	0.0080	
		50	5e	0.005	0.003	0.004	0.004	0.004	0.006	0.005	0.013	0.0055	0.007
			5b	0.066	0.036	0.021	0.041	0.001	0.039	0.025	0.026	0.0255	0.002
			5d	0.004	0.004	0.006	0.005		0.009	0.009	0.007	0.0083	
		100	6a	0.016	0.02	0.018	0.018	0.017	0.023	0.026	0.027	0.0253	0.024
			6b	0.026	0.044	0.03	0.028	0.010	0.037	0.039	0.035	0.0370	0.011
			6c	0.004	0.004	0.004	0.004		0.009	0.01	0.016	0.0095	
pH 7.5	Low Algae	20	7a	0.032	0.032	0.032	0.032	0.003	0.087	0.084	0.084	0.0850	0.056
			7b	0.001	0	0.002	0.001	0.003	0.044	0.046	0.047	0.0457	0.022
			7d	0.007	0.005	0.004	0.005		0.04	0.037	0.036	0.0377	
		50	8f	0.003	0.002	0.006	0.004	0.005	0.009	0.01	0.011	0.0100	0.010
			8b	0.007	0.004	0.004	0.005	0.002	0.139	0.13	0.139	0.1360	0.001
			8e	0.006	0.005	0.008	0.006		0.01	0.012	0.01	0.0100	
		100	9a	0.033	0.019	0.018	0.023	0.019	0.027	0.025	0.025	0.0257	0.023
			9b	0.028	0.031	0.032	0.030	0.013	0.027	0.03	0.032	0.0297	0.007
			9c	0.007	0.002	0.003	0.003		0.012	0.014	0.012	0.0127	
	High Algae	20	10a	0.034	0.034	0.042	0.034	0.003	0.058	0.056	0.052	0.0553	0.053
			10d	0.001	0.001	0.001	0.001	0.002	0.026	0.023	0.023	0.0240	0.024
			10c	0.004	0.006	0.006	0.005		0.083	0.076	0.076	0.0783	
		50	11d	0.013	0.003	0.001	0.002	0.003	0.015	0.012	0.01	0.0123	0.013
			11b	0.005	0.009	0.004	0.005	0.001	0.016	0.015	0.014	0.0150	0.002
			11c	0.004	0.003	0.004	0.004		0.011	0.012	0.012	0.0117	
		100	12a	0.043	0.047	0.042	0.044	0.005	0.05	0.047	0.054	0.0485	0.026
			12b	0.009	0.007	0.007	0.008	0.003	0.016	0.018	0.041	0.0170	0.018
			12c	0.002	0.001	0.002	0.002		0.012	0.011	0.019	0.0115	